ASSESSING THE USE OF IMAGERY FROM SENTINEL-2 AND AN UNMANNED AERIAL VEHICLE TO MONITOR NYMPHOIDES PELTATA IN AN OKLAHOMA RESERVOIR

By

ABIGAIL A MCCREA

Bachelor of Science in Environmental Science

Northern Michigan University

Marquette, Michigan

2017

Submitted to the Faculty of the
Graduate College of the
Oklahoma State University
in partial fulfillment of
the requirements for
the Degree of
MASTER OF SCIENCE
May, 2020

ASSESSING THE USE OF IMAGERY FROM SENTINEL-2 AND AN UNMANNED AERIAL VEHICLE TO MONITOR NYMPHOIDES PELTATA IN AN OKLAHOMA RESERVOIR

Thesis Approved:

Scott Stoodley

Thesis Adviser

Andrew Dzialowski

Ranjeet John

Hamed Gholizadeh

ACKNOWLEDGEMENTS

I would like to thank my friends, family, and colleagues. A special thank you to lab mates Stephen Angle, Caleb Biles, Kavina Eksteen, Benjamin Lamb, Meghan Martin, and the pilot Victoria Natalie. Without all of your advice and support this research truly would not have been possible. Thank you to my committee members for your direction and patience.

Name: ABIGAIL A MCCREA

Date of Degree: MAY, 2020

Title of Study: ASSESSING THE USE OF IMAGERY FROM SENTINEL-2 AND AN UNMANNED AERIAL VEHICLE TO MONITOR NYMPHOIDES PELTATA IN AN OKLAHOMA RESERVOIR

Major Field: ENVIRONMENTAL SCIENCE

Abstract: Remote sensing of aquatic invasive plants has been relatively understudied for treatment monitoring applications. Invasive aquatic plants cause ecological distress as well as millions of dollars in damages and lost utility value and ecosystem services. Yellow floating heart (*Nymphoides peltata*) is a floating leaved macrophyte native to Southeast Asia and the Mediterranean. This plant has prolific spread potential and can create dense canopies that shade out other organisms. It was reported in Lake Carl Blackwell of Oklahoma in 2014. It covered over 20 hectares at its peak in 2019. The herbicide ProcellaCOR was applied to the infestation in the summer of 2019. The purpose of this research was to use Sentinel-2 satellite data and an unmanned aerial vehicle equipped with a MicaSense RedEdge-M camera to monitor the infestation and compare the sensors from spatial and spectral parameters. This can help lake managers integrate remote sensing tools into their monitoring programs in a cost-effective manner. A Sentinel-2 dataset was downloaded from the USGS EarthExplorer. UAV data was collected and processed in AgiSoft Structure-from-Motion. The Sentinel-2 and UAV datasets were classified by Maximum Likelihood Classification to compare ability to detect and delineate *N. peltata* with overall accuracies of 96.1% (kappa = 0.88) and 94.3% (0.80), respectively. The spatial extent was manually digitized on all available data and compared with regression analysis with a significantly high relationship ($R^2 = 0.94$; $p < 0.001$). This measure also indicated a 91% reduction of the infestation after the herbicide application, a reduction of almost 2% lake coverage to less than 0.1%, due to herbicide treatment. The sensors were also compared in their measurements of the Normalized Difference Vegetation Index ($R^2 = 0.40$; $p = 0.13$) and the Fractional Vegetative Index ($R^2 = 0.39$; $p = 0.13$) both of which had low significance. The spatial data from Sentinel-2 was used to make an estimation of the potential economic impact caused by this infestation by correlating it to the average lake value.

TABLE OF CONTENTS

Chapter Page

LIST OF TABLES

Table Page

LIST OF FIGURES

Figure Page

CHAPTER I

INTRODUCTION

Remote sensing has been used since the 1970's to image changes in vegetation (Lillesand, Chips & Keifer, 2015). Studies typically focused on measuring crop parameters with black and white aerial imagery or color infrared aerial imagery. Imaging platforms have evolved over time to include satellites and small unmanned aircraft equipped with multispectral cameras. Multispectral data can improve classification of plant species and estimate biological parameters like plant health and density (EO NASA, 2000). Remote sensing benefits include repetitive data collection over large survey areas. This reduces labor costs compared to field surveys (Villa et al., 2018). Remote sensing is used in precision agriculture to detect basic biological parameters that would indicate the presence of weeds and disease (Lukas et al., 2016). Fewer applications have been executed for invasive plants in aquatic ecosystems (Gao et al., 2017; Joshi et al., 2004; Villa et al., 2015).

The negative impacts of invasive species cost the United States an estimated $120 billion annually in damages and management costs (Pimentel et al., 2005). The magnitude of costs incurred from individual invasive species varied widely based on the level of infestation, scale of treatment, and applied methods (Marbuah et al., 2014). The introduction of non-native species can have major impacts on ecosystem stability by interrupting nutrient cycles, outcompeting native species, affecting hydrology, or changing the physical structure of the environment

(Kovalenko & Dibble, 2011; Simberloff, 2015). Invasive species often inhibit the use and value of natural resources for commercial and recreational purposes (Cacho, 2007).

The aquatic invasive plant Yellow floating heart (*Nymphoides peltata)* invaded Lake Carl Blackwell, which is a popular recreation area in north central Oklahoma. The infestation grew to cover over 20 ha in 2018 (Angle, 2019). The reservoir was treated in July of 2019 with the herbicide ProcellaCOR. The large expanse of the plant in monospecific mats and claims of short-term results by the herbicide manufacturers made this an ideal study for using remote sensing.

Monitoring in environmental projects is usually lacking because field surveys are laborious and costly (Lovett et al., 2007). Remote sensing offers a unique tool to survey land area quickly. The chosen sensor should be of appropriate scale resolution to measure the desired feature (Lillesand, Chips, & Keifer, 2015). Satellites and unmanned aerial vehicle (UAV) have benefits and limitations that affect their use in projects like vegetation monitoring. This study compares the open-source satellite Sentinel-2 to a UAV equipped with the multispectral, MicaSense Red Edge camera to monitor *N. peltata* over the summer of 2019.

Imagery from both sensors were used in a Maximum Likelihood Classification to determine how well they could detect and classify *N. peltate*. The multispectral imagery was used to delineate the spatial coverage of the infestation and to calculate the Normalized Difference Vegetation Index (NDVI) (Jackson et al., 1983) with a simple workflow. The NDVI results were then used to calculate the pixel Fractional Vegetative Coverage (Song et al., 2017). The results from these analyses from the two platforms were compared to one another with linear regression to determine if they produce similar outcomes.

The objectives of this study are to:

1. Compare accuracy to detect/classify *N. peltata* between sensors.

2. Measure plant response parameters (spatial extent, Normalized Difference Vegetation Index, Fractional Vegetative Cover) to herbicide treatment and compare between sensors.

3. Estimate the potential loss of use value to Lake Carl Blackwell due to *N. peltata*.

CHAPTER II

LITERATURE REVIEW

Remote Sensing and Spatial Analysis

Field surveys are often time-consuming, expensive, logistically challenging, and labor intensive. The development of satellite platforms has made it possible to gather repetitive imagery over large swaths of land. Most satellite platforms use multispectral cameras of varying spectral and spatial resolutions (Lillesand, Chips, & Keifer, 2015). This type of tool is ideal for monitoring vegetation and has gained attention for its utility to detect and observe invasive plants (Bradley, 2014; Husson, Hagner, & Ecke, 2014) and aquatic plants (Silva et al., 2008). Frequent high-resolution imagery has been too costly for most environmental projects until recently (Villa et al., 2018). All sensors continue to be limited to some degree by spectral, spatial or temporal resolutions, and poor weather conditions.

Innovations in platform and sensor technology have improved upon some of these limitations with open-source satellite imagery and unmanned aerial vehicles (UAV) equipped with multispectral cameras. Benefits of UAV include access to hard to reach areas, flexible data collection, and reduced labor. Limitations include battery power, range, high costs, and required technical knowledge (Husson, Hagner, & Ecke, 2014).

Interest for environmental projects like invasive plant detection or treatment monitoring revolve around spatial resolution for estimating spread and coverage, and spectral resolution for

species classification and plant index calculation. It is possible to detect vegetation when there is sufficient spatial coverage, unique phenological or structural characteristics (Huang & Asner, 2009; Penuelas et al., 1993). Scale resolution is an important aspect for environmental monitoring to choose the appropriate tool for different projects (Dash et al., 2018; Lukas et al., 2016; Mullerova et al., 2013).

Sentinel-2

The European Space Agency (ESA) launched the Sentinel-2 mission 2015 (Sentinel-A) and 2017 (Sentinel-B) as part of a program to provide high quality open-source data for earth observation. These two satellites have a return period of five days. The Multispectral Instrument (MSI) on board records thirteen spectral channels at 10, 20, and 60m (Table 1). The visible region (0.490 – 0.665 ɥm) and the Near Infrared Red (NIR) bands have 10m resolution. This sensor is unique in that it records four distinct channels of the Red Edge at 20m (Suhet, 2015).

Imagery can be downloaded from the ESA Copernicus open-access HUB, or from the United States Geological Survey (USGS Earth Explorer, 2019) data viewer. This satellite produces image tiles approximately 100 x 100 km^2 in UTM/WGS84 projection. The data for download must be pre-processed to Bottom-of-Atmosphere (BOA) imagery by applying atmospheric, terrain, and cirrus corrections (De Keukelaere et al., 2017). ESA provides an open-source pre-processing software called the Sentinel Application Platform (SNAP) for users to apply these corrections to their downloaded data.

Table 1. Spatial and spectral resolutions of the bands of the Multispectral Instrument sensor on board Sentinel-2 satellites (ESA, 2019).

Spatial Resolution (m)	Band Number	S2A		S2B	
		Central Wavelength (nm)	Bandwidth (nm)	Central Wavelength (nm)	Bandwidth (nm)
10	2	492.4	66	492.1	66
	3	559.8	36	559.0	36
	4	664.6	31	664.9	31
	8	832.8	106	832.9	106
20	5	704.1	15	703.8	16
	6	740.5	15	739.1	15
	7	782.8	20	779.7	20
	8a	864.7	21	864.0	22
	11	1613.7	91	1610.4	94
	12	2202.4	175	2185.7	185
60	1	442.7	21	442.2	21
	9	945.1	20	943.2	21
	10	1373.5	31	1376.9	30

MicaSense Red Edge Camera

The MicaSense RedEdge-M is a multispectral camera that records across five wavelengths (Blue, Green, Red, Near IR, Red Edge). It records at a ground sample distance of 8.2 cm per pixel, per band at 120 m altitude. Its spectral resolution ranges from 400 to 900 nm (MicaSense, 2019).

Table 2. Spatial and spectral resolutions of the bands comprising the MicaSense RedEdge-M multispectral camera (MicaSense, 2019).

Band Number	Band Name	Center Wavelength (nm)	Bandwidth FWHM (nm)
1	Blue	475	20
2	Green	560	20
3	Red	668	10
4	Near IR	840	40
5	Red Edge	717	10

Classification

Computer-based classification helps detect unwanted species earlier, improving control of invasive plants while reducing labor and costs (Hestir et al., 2008). Supervised classification methods, like the Maximum Likelihood Classification method, rely on spectral classes created by a human to train the computer to identify certain spectral patterns. The computer then assesses each pixel in an image for the statistical likelihood that it belongs to a particular class (Lillesand, Chips, & Kiefer, 2015). Pixel-based analysis has been shown to have higher accuracies than computer-based classifications compared to reference data (Belgiu & Csillik, 2018; Faidi, Hasson, Shamasuddin, 2018; Husson, Ecke, & Reese, 2016).

Scale resolution has been shown to have significant impacts on classification accuracy (Mullerova et al., 2013). Luo et al (2016) used 30m Landsat TM imagery to measure seasonal and interannual variation of aquatic vegetation types. They used a classification tree calibrated with aquatic vegetation indices demonstrating some moderate to high accuracies. Villa et al (2015) performed a similar analysis concluding macrophyte communities can be mapped with medium resolution data (10 – 30m; 400 – 900nm) with different vegetation indices. Their results had overall accuracy of 90.41% with less than 20% error for each class.

Maximum Likelihood Classification (MLC) is a common method in remote sensing analysis (Lillesand, Chips, & Keifer, 2015; Faidi, Hasan, & Shamsuddin, 2018). Valta-Hulkkonen, Kanninen, and Pellikka (2004) used aerial imagery with different spectral and spatial

resolutions and processed them with MLC to relate the ground measurements of Common club-rush (*Schoenoplectus lacustris*) to reflectance values before and after an ecosystem restoration project. They estimated a 30% decrease of biomass that was highly correlated ($R^2 = 0.889$, $p < 0.001$) to ground measurements measured in a GIS environment. A study in Lake Tasik Chini used Sentinel-2 imagery to discriminate land use/land cover and identify distributions of Indian lotus (*Nelumbo nucifera)* using Maximum Likelihood (Faidi, Hasan, & Shamasuddin, 2018). They estimated that their analysis yielded 89% accuracy.

Hill et al (2017) mapped the invasive Yellow flag iris (*Iris pseudacorus* L.) in their study area by three methods: field, manual image interpretation, and image classification of UAV imagery. They concluded that manual digitization in a GIS environment was often more accurate and faster than pixel-based classification methods. This was true when identifying large monospecific stands of vegetation (Silva et al., 2008), but is more time consuming with increased complexity (Husson, Ecke, & Reese, 2016).

Measuring Biological Parameters

Measuring vegetation spatial extent over time is a common application in remote sensing. It can be useful for defining treatment areas and estimating project costs. It also helps direct management practices like herbicide treatments, fertilizer application, and watering regimes (Joshi et al., 2004). It is essential to be able to quickly and accurately make these types of estimates, since control needs change over the course of a season. Spatial measurements have been used to correlate vegetation models to ground observations (Ma et al., 2008; Matese et al., 2017).

Analysis of multispectral imagery is an effective method for researchers to estimate many biological parameters of vegetation. Several reviews of remote sensing studies of invasive plants found that non-native species were often distinguishable from natives based on novel text,

biochemistry, growth patterns or phenological differences (Huang and Asner, 2009; Bradley, 2014). Parker Williams & Hunt (2002) mapped the invasive Leafy spurge (*Euphorbia esula*) in North American rangelands using high resolution airborne imagery. Using a spectral mixture analysis, they found the distinctive color of Leafy spurge was spectrally unique from native prairie and forest species so that it could be detected remotely.

Spectral distinctions of vegetation are analyzed using vegetation indices. The most common vegetation index is the Normalized Difference Vegetation Index (NDVI) (Jackson et al., 1983). It is used as a way to measure photosynthetic activity through chlorophyll production. NDVI is a ratio of the red and near-infrared (NIR) channels of multispectral measurements. It determines the density of green (chlorophyll) within a pixel and has been strongly correlated to plant biomass, percent canopy cover, density, and health (Villa et al., 2014; Ma et al., 2008; Penuelas et al., 1993; Wang, Sun, & Liu, 2012).

Farid Muhsoni et al (2018) analyzed 24 spectral indices calculated from Sentinel-2 imagery to measure density of mangrove forests and determined NDVI could most accurately estimate biomass and canopy density along a coastline. Henick (2012) used NDVI to monitor crop stress from management practices. The author found that NDVI changed over different life stages and that it could predict crop yield. Duan et al (2017) found that NDVI measured with the MicaSense RedEdge M were highly correlated to field plot sensor measurements to differentiate wheat cultivars.

NDVI can be used to calculate biological parameters such as fractional vegetative cover (FVC) (Song et al, 2017). FVC estimates what percent of the pixel signal is from vegetation and can be a proxy for estimating biomass or density. This formula indexes the NDVI with its lowest value (soil) and highest value (healthy vegetation). The result is a measurement that reflects the percent of chlorophyll productivity in a pixel that should reduce the influence of non-vegetative

signals. Imagery without a NIR channel can still be used to measure FVC, but instead of the NDVI the Visible Atmospherically Resistant Index (VARI) is used. Gitelson (2002) developed this index to use the visible range reflectance to estimate the amount of green reflectance in a pixel as a proxy to estimate plant health. The results of this index can then be used in the FVC equation.

Aquatic ecosystems pose an extra challenge in remote sensing analyses (Wang et al., 2012). Open water strongly absorbs red and NIR electromagnetic radiation, whereas plants strongly reflect in the NIR. Signatures from different aquatic plant types (submerged, floating and emergent) have key differences that are due to the depth at which they grow and the influence of water (Penuelas, 1993). Water strongly absorbs red and NIR electromagnetic radiation, so the presence of water can interfere with radiometric signal of submerged or floating vegetation (Kaplan & Avdan, 2017; Ma et al., 2018; Villa et al., 2018; Silva et al., 2008).

Multi-Platform Studies

Remote sensing tools come in a wide range of spatial, spectral, and temporal resolutions. Landsat has spatial resolutions of 15 to 60 m and a return time of 16 days. This is great for monitoring global patterns, but is not necessarily useful for small scale studies. New sensor technology and platforms are being developed that increase resolution and should be evaluated for their use in environmental projects. Recent studies correlate sensors by scaling their measured parameters to one another to determine if they produced similar results.

Dash et al (2018) estimated forest health with a modified NDVI using UAV (MicaSense RedEdge 3) and RapidEye ($6.5m^2$) satellite imagery to detect physiological stress in trees from herbicide treatment. They carried out time-series analyses of different vegetation indices in ArcMap and correlated them to images from both sensors using regression models. They found that both sensors had significant capability to detect plant stress from various indices. Lukas et al

(2016) did a correlation analysis of vegetation indices using UAV and Landsat Operational Land Imager. Their results showed positive correlation to field measurements, but each sensor had specific limitations that affected their success for monitoring.

Nymphoides peltata

Nymphoides peltata is an invasive freshwater plant that was first reported at Lake Carl Blackwell (LCB) Oklahoma in 2014. It is native to Eurasia and the Mediterranean and considered invasive in several countries including the United States. Commercial sale and export of *N. peltata* has been considered the primary method of dispersal to new water bodies.

Nymphoides peltata reproduces via fertilization, vegetative expansion, fragmentation, or colonizing propagules. Flowering occurs from June to October in North America. Flowers are bright yellow with 5 fringed petals that are 3 – 4 cm in diameter. Fruit pods are 1.2 – 2.5 cm wide capsules after pollination (Darbyshire & Francis, 2008). Van der Velde & Van der Heijden (1981) reported an average density of 180 fruits/m^2 in a Swedish infestation. Fruits contain 40 – 80 elliptical seeds. They are 4 – 5 mm in length and have trichomes that form interlocking chains of floating seeds (Nault & Mikulyuk, 2009). Trichomes may aid in dispersal by allowing seeds to adhere to waterfowl and foraging wildlife that travel between waterbodies (Cook, 1990). Seeds require certain conditions for germination as *N. peltata* is generally limited to well buffered waters with mineral substrates, such as clay (Van der Velde, 1979). Seeds can withstand significant desiccation (Smits, et., 1988), but need high oxygen and light levels to germinate.

This plant forms complex structures composed of rhizomes, stolons, leaves and adventitious roots. Shoots can become heart-shaped leaves 3 – 15 cm in diameter that are bright green and have slightly scalloped margins (Brock et al., 1983; Grosse & Mevi-Schutz, 1987). Huang et al (2014) measured the buoyancy of *N. peltata* seeds and germination rates in response to environmental factors and concluded that vegetative expansion contributes more to area

colonization. Zhonghua et al (2007) reported that a single plant can produce over 100 new plants in 12 weeks from their rhizomes.

Nohara (1991) used aerial imagery to measure the rate of spread of *N. peltata*. They found *N. peltata* could expand its spatial extent vegetatively from 3.8 – 10.0 m/year in any one direction. This rate of expansion could be overwhelming and have negative effects, especially in smaller waterbodies. Colonization of new areas of a waterbody are attributed to fragments or propagules. *Nymphoides peltata* can form a new individual from plant fragments that have at least one node (Darbyshire & Francis, 2009). This makes physical removal extremely challenging and could have contrary effects.

Nymphoides peltata in the United States

The United States Department of Agriculture and Plant Health Inspection Service assessed the invasive potential of *N. peltata* and rated it a High-Risk species due to its ecosystem impacts and establishment/spread potential (USDA APHIS, 2012). Infestations have been confirmed in 32 states and is designated as a noxious weed in Connecticut, Maine, Massachusetts, Oregon, Vermont, and Washington (NRCS, 2019; ODA, 2018). The introduction and dispersal of non-native species is largely attributable to economic activities in trade and transport (Lovell & Stone, 2006). *Nymphoides peltata* is introduced to new areas anthropogenically. It is not federally regulated as a noxious weed and can be commercially grown and sold, often as an ornamental.

States have individual noxious weed lists and develop invasive species management plans. Oregon has added YFH to the state Noxious Weed List to reduce introduction. The Oregon Department of Agriculture recommend physical removal in small ponds. Their studies suggest that endothall, diquat, imazamox and imazapyr could be effective treatment options (ODA, 2018).

The Massachusetts Office of Coastal Zone Management wrote the MA Aquatic Invasive Species Management Plan, mentioning YFH as a species to be aware of. It has not been updated

or supplemented since 2002 and does not provide specific management advice (MA OCZM, 2002). Other states have not provided official plans to find and eradicate *N. peltata*.

There is no commercial regulation of YFH in Oklahoma and it is not on the Oklahoma noxious species list (PLANTS USDA, 2019). YFH has been previously reported in Oklahoma ponds located in McCurtain county in 1948 and 1958. It was also reported in Lake Texoma in 1947 (USGS NAS, 2019). These populations are no longer present. YFH was discovered in the Lake Carl Blackwell reservoir in Payne County, Oklahoma in 2014.

Nymphoides peltata in Other Countries

Countries such as Ireland, New Zealand, Canada, and Sweden have had infestations of *N. peltata* and all have designated it as a pest or noxious weed (Nault & Mikulyuk, 2009). It has been confirmed in 16 Irish waterbodies. They plan to create the Ireland Invasive Species Action Plan for *N. peltata.* This will outline how to limit the impact of the plant by preventing new introductions and establishing eradication methods. Policies have been put in place to restrict sales of non-native species in order to prevent invasive species expansion. They also plan to take steps to increase public awareness of the negative impacts of non-native plants and to promote native species (Kelly & Maguire, 2009).

New Zealand claims eradication of *N. peltata* in its boundaries. They continue to manage it by banning its sale distribution. They harvest newly found infestations until its coverage is zero (Champion, Hofstra, & Winton, 2019).

Nymphoides peltata was first planted in the Arbogaan River in Sweden in 1933 and has since spread to around 40 waterbodies. Control measures include mechanical harvesting and chemical treatments. Neither of these treatment options have been considered successful (Carlsson & Kataria, 2008).

Populations of *N. peltata* have been reported in the Canadian provinces: Ontario, Quebec, British Columbia, Nova Scotia, and Newfoundland and Labrador. Canada has strict aquatic herbicide use restrictions, so they recommend landowners use physical control methods. It is suggested that draining and allowing the soil to dry sufficiently may destroy the seedbed in smaller waterbodies. Benthic barriers may also be an alternative or additional measure (Darbyshire & Francis, 2009).

Control of *Nymphoides peltata*

Oregon Department of Agriculture Noxious Weed Program tried multiple methods to eradicate a 1.2-acre YFH infestation in Willow Sump, Umpqua National Forest. Initially they attempted physical removal, which took place over three weeks. One month later the infestation had completely regenerated. Benthic barriers were tested and after two years were removed and had promising results, however, in their ecosystem the presence of willow trees made widespread use impractical. They subsequently chose to apply an herbicide known as Imazapyr, which yielded a 95% reduction in the following year (ODA, 2018).

Zhu et al (2019) studied the impacts of mechanical YFH removal at Lake Taihu in China. Over 196 km^2 of vegetation was removed using machinery. They found that re-establishment next year ranged from 29 – 95% of the previous extent and that success rates varied by the month removal took place.

A treatment by the Florida Collier County Storm Water Management achieved partial control of Crested Floating Heart (*Nymphoides cristata*, CFH). They used an application combination of glyphosate and imazapyr. The herbicides reduced foliar coverage, but after four weeks the infestation had regenerated (Willey & Langeland, 2018).

Crested Floating Heart is of the same genus as *Nymphoides peltata* and would share many physiological traits, including a similar response to a hormone-based herbicide. Beets and

Netherland (2018) conducted an outdoor mesocosm study to measure the response of invasive plants Hydrilla and CFH and two native species to florpyrauxifen-benzyl (FPB). They were testing concentration dose and exposure time to biomass reduction, as well as water column concentration. After 24 hours, the concentration of FPB or byproducts were below detectable limits. Hydrilla biomass declined 68 – 80% after 28 days and CFH biomass declined 89 – 100%. The amount of biomass affected was positively correlated to the length of exposure time, but there was no significant increase in control when doubling concentrations from 24 to 48 ug/L. The native species *Sagittaria lancifolia* was not impacted by FPB, but the pickerel weed was nearly eliminated.

ProcellaCOR

Lake Carl Blackwell management planned to treat their infestation of *N. peltata* with the herbicide ProcellaCOR in July 2019 (Angle, 2019). The active ingredient of ProcellaCOR is florpyrauxifen-benzyl and was developed by the SePRO corporation with Dow Agrosciences (MDA, 2018). It is a Weed Science Society of America Group 4 herbicide. This means it interferes with plant reproduction and growth processes. It has only been on the market for approximately two years at the time of study. It had been previously tested for ecological impacts for over eight years before being approved for use the EPA. (SePro, 2019).

The US EPA classified ProcellaCOR as a Reduced Risk herbicide due to its short residence time and half-life in water (2 – 6 days). There are no known health risks to wildlife or people from bodily exposure (MDA, 2018). ProcellaCOR has been used to successfully treat infestations of *N. peltata* and several other invasive aquatic weeds (e.g., hydrilla and milfoil) in 12 states (SePRO, 2019). The producers estimate complete reduction of *N. peltata* 6 – 8 weeks after application with no adverse impacts on water quality or native taxa.

Beets and Netherland (2018) conducted an outdoor mesocosm study to measure response to dose concentration and exposure time from invasive plants Hydrilla and CFH to florpyrauxifen-benzyl (FPB). The concentration of FPB or byproducts were below detectable limits within 24 hours. Hydrilla biomass declined 68 – 80% after 28 days and CFH biomass declined 89 – 100%. The amount of biomass affected was positively correlated to the length of exposure time.

Economic Review

The introduction and dispersal of non-native species is largely attributable to economic activities in trade and transport (Lovell & Stone, 2006). Many articles have emerged that estimate the damage costs of invasive species in the US in recent years. These estimates vary widely from <$1 million USD to 12% of the gross domestic product (Marbuah et al, 2014). It is necessary to have an accounting of bioeconomic features like spread, control, and damage processes to estimate established invader damage impacts (Epanchin-Niell & Hastings, 2010). A literature review by Marbuah et al (2014) concluded most studies of invasive species control failed to monitor the results of their chosen strategy. This was confirmed by a review conducted by Ketternring and Adams (2011).

There are three essential components to link economics and invasive plant management: knowledge of plant control and populations, plant populations and lake use, lake use and lake-based value (Adams & Lee, 2007). Florida state agencies used preference surveys to measure angler willingness-to-pay for the removal of invasive aquatic plant cover. Adams and Lee (2007) used these survey results and known invasive plant coverages of water hyacinth, water lettuce, and hydrilla in 13 waterbodies. They established an empirical bioeconomic model by using observations of plant coverages, control costs, fishing activity and lake characteristics as

simulated control. They used this to estimate potential lost fishing benefits from $64.78 million per year on 13 waterbodies.

CHAPTER III

METHODOLOGY

Analyses of this study were carried out under the same geographic and projection coordinate systems (WGS 84 UTM Zone 14N) to ensure comparable measurements. Satellite and UAV images were clipped to the hydrogeologic extent of Lake Carl Blackwell to maintain the same number of rows and columns for analysis. A dataset of satellite and UAV imagery from 2019 was first processed with the Maximum Likelihood Classification (MLC) to determine the detectability of *N. peltata* at the respective sensor resolutions. The same dataset was then visually assessed to determine the spatial extent of the vegetation. This was followed by spectral analyses to calculate the NDVI and FVC. Regression analysis was performed for a dataset of temporally corresponding dates of the satellite and UAV data. A dataset from 2018 composed of Sentinel-2 and RGB UAV imagery was validated using ground measurements. An estimation of the economic impact of *N. peltata* at Lake Carl Blackwell was conducted following spectral analyses.

Study Area

Lake Carl Blackwell is a 1,300-ha reservoir with an average depth of 4.9 m located in north central Oklahoma (36.1344 N, 97.2302 W) (Figure 1) (Toetz, 2009). The reservoir is in a watershed that is characterized by agricultural production. Soils are composed of sandy, silty loam and generally have high clay content (Howick & Wilhm, 1985). Average annual temperatures range between 9°C and 34°C. Annual precipitation averages 96.52 cm (OK EPSCOR, 2019). Most of the *N. peltata* infestation was located in the north central arm of the

reservoir. It dominated areas along the shoreline and smaller inlets (Angle, 2019). The satellite records data for the entire lake but the UAV was limited to smaller areas. An area referred to as Cove D is where the multispectral UAV imagery was captured in 2019 (Figure 1).

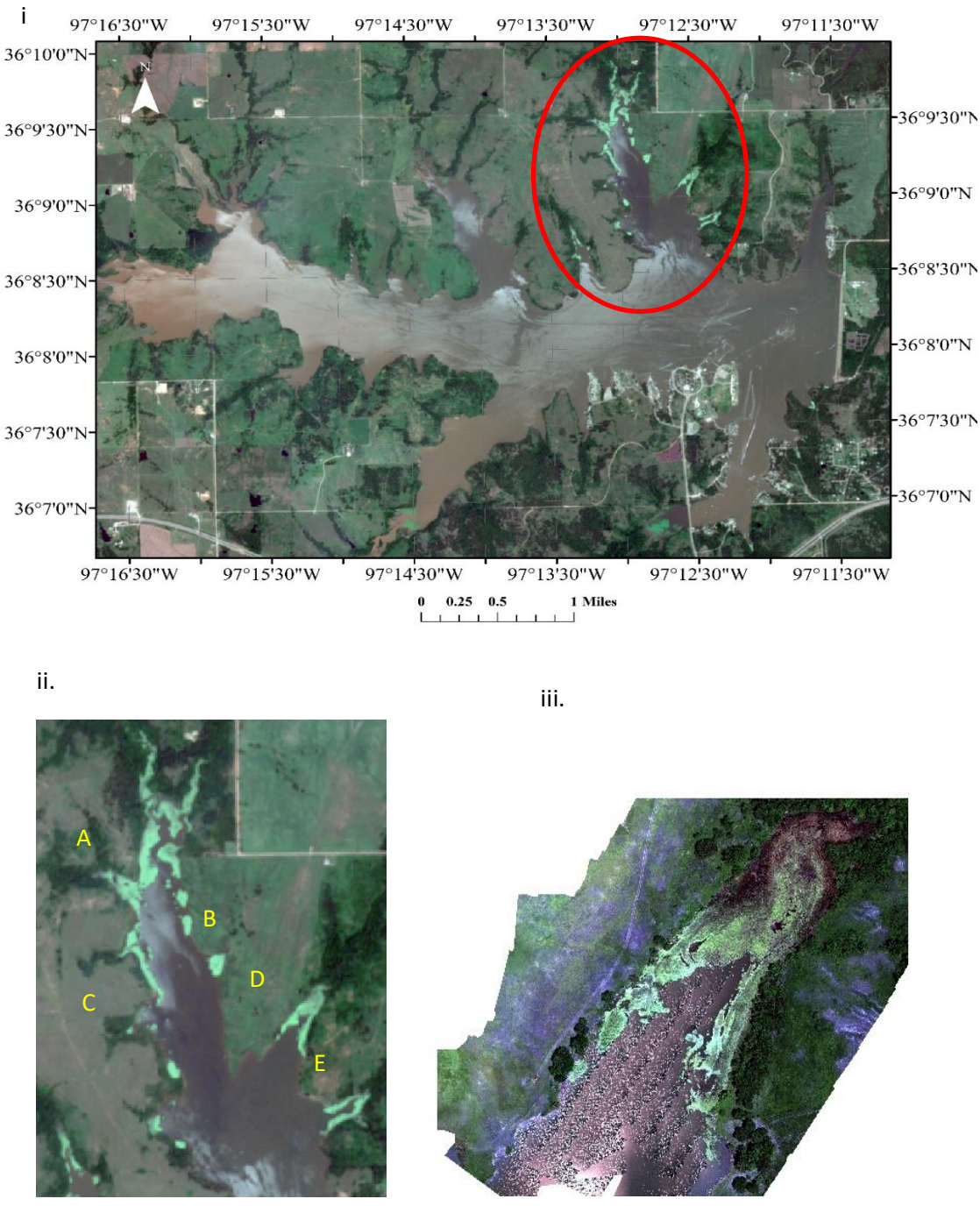

Figure 1. Lake Carl Blackwell is the study location. The top image is Sentinel-2 imagery (6-29-19). On the bottom left is the inlet containing the majority of the infestation and the red circles indicate where

field data was collected. The image on the bottom right is a UAV image (7-11-19) and defines the observation area known as Cove D.

Data Collection and Preprocessing

Sixteen Sentinel-2 images were downloaded from the USGS Earth Explorer from May – October 2019 for use in this study (Table 3). Images of the location Tile T14SPF were selected based on the visibility of the study area. Images where more than 10% of the infestation was obscured by clouds were excluded from analysis. All data were pre-processed to Bottom of Atmosphere (BOA) reflectance using the ESA program SNAP and the Sen2Cor plugin v 7.0.0. This is a necessary pre-processing step in order to correct for atmospheric distortion. Only 10 m bands 2, 3, 4, and 8 (Table 1) were used for image classification.

Table 3. Sentinel-2 (n = 16) and UAV (n = 12) imagery collection dates from 2019, Tile T14SPF and the study area, respectively. Dates denoted with (*) are used for direct comparisons between the two sensors.

Day of Year	Sentinel-2	UAV	Day of Year
150	5/30/2019	*6/12/2019	163
160	*6/9/2019	*7/11/2019	192
175	6/24/2019	7/17/2019	198
180	6/29/2019	*7/19/2019	200
190	*7/9/2019	*7/24/2019	205
200	*7/19/2019	7/25/2019	206
205	*7/24/2019	7/29/2019	210
210	*7/29/2019	*7/31/2019	212
240	*8/28/2019	8/7/2019	219
250	*9/7/2019	8/14/2019	226
260	9/17/2019	*8/28/2019	240
270	9/27/2019	*9/11/2019	254
290	10/17/2019		
295	10/22/2019		
300	10/27/2019		

A MicaSense RedEdge Multispectral camera mounted to drone model DJI Matrice-100 was used to collect spectral data from Cove D (Figure 1). It was collected 12 times between June and September 2019 (Table 3). The imagery was composed of five bands (Table 2) (Red, Green, Blue, NIR, RE) and had a spatial resolution of approximately 8 cm. The UAV was flown to

correspond with Sentinel-2 satellite overpass dates as often as possible. Orthomosaics of the scene were generated using the Structure-from-Motion algorithm in AgiSoft PhotoScan mapping software (Figure 2). Seven dates from Sentinel-2 and the Red Edge that correspond temporally were selected for comparisons of *N. peltata* spatial coverages, NDVI, and FVC using linear regression (Table 2).

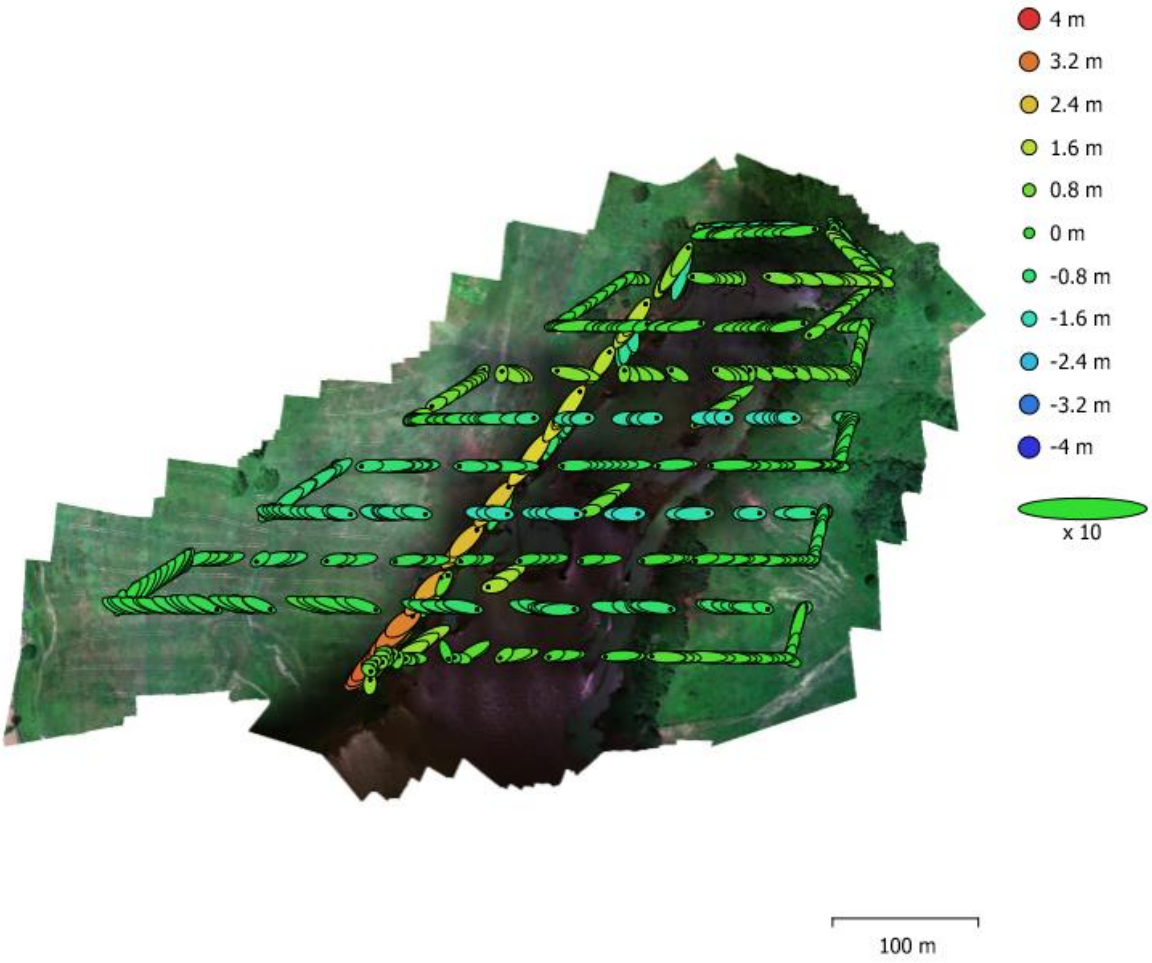

Figure 2. Example of UAV orthomosaics of Cove D composited with AgiSoft Structure-from-Motion. Dots indicate the camera location upon capture and oblong shapes are error estimates that range from -4 to 4 m.

Image Analysis

The workflow (Figure 3) for the satellite and UAV data followed these steps: (1) pre-process satellite data to BOA reflectance and composite aerial photos into orthomosaics; (2) Maximum Likelihood Classification and accuracy assessment which involves the creation of

training and validation regions of interest (ROI); (3) Processing data, includes hand-digitizing the spatial extent of *N. peltata*, the generation of multitemporal NDVI and FVC datasets; (4) Comparison of the results obtained from these two datasets with different resolutions using regression analysis. Validation was done by overlaying field sampling points from 2018 over FVC computed from UAV and Sentinel-2 imagery collected in 2018.

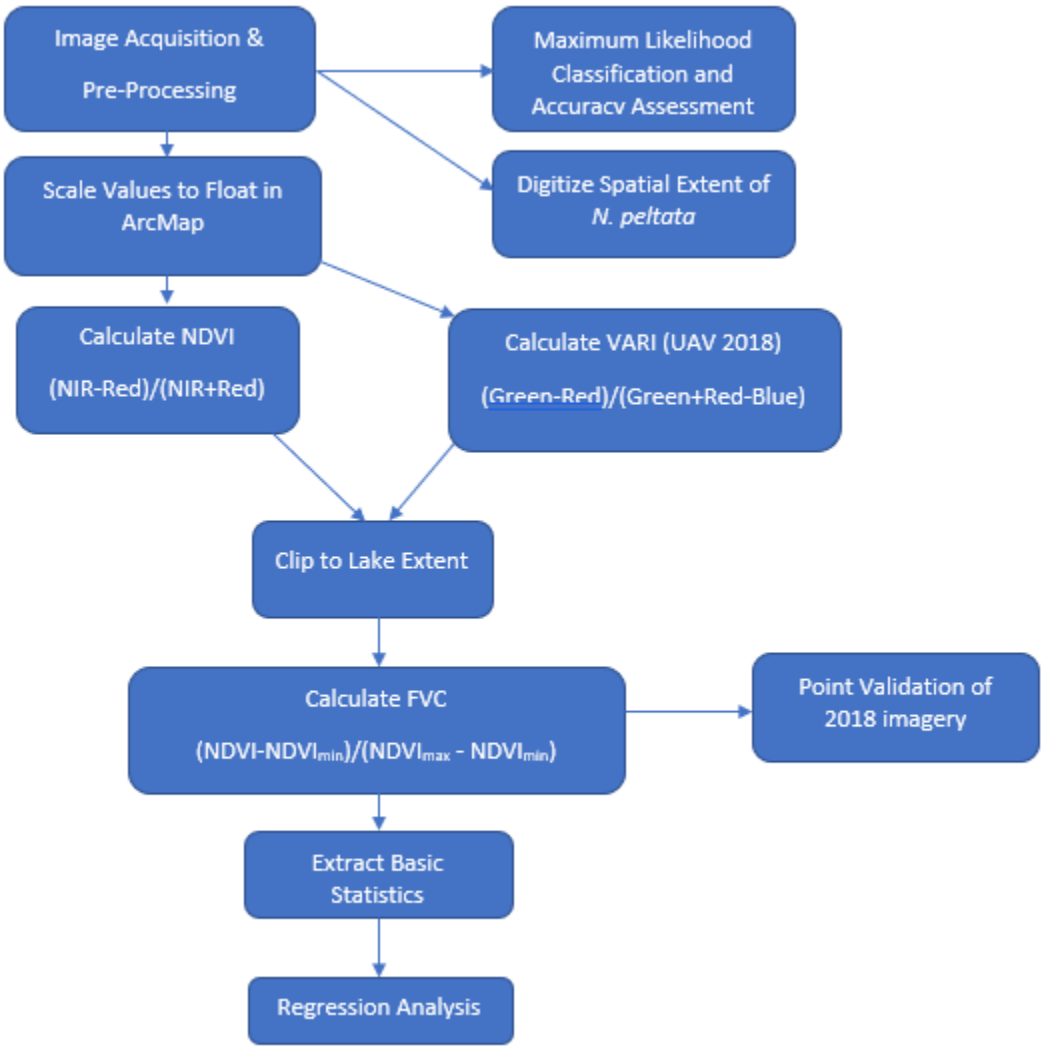

Figure 3. Illustration of the workflow used to compute spectral indices and extract their values from multi-temporal datasets. All collected images were processed using this method.

Supervised Classification and Accuracy Assessment

The MLC was carried out in the ENVI image analysis software package (Harris Geospatial, 2019) on all image dates found in Table 2. Training and validation datasets were created from ROIs for each date. Classes were (1) *N. peltata*, (2) other vegetation (OV), and (3) water. All satellite and UAV image were clipped to the boundary of Lake Carl Blackwell so that only the pixels within the hydrogeologic boundary were classified.

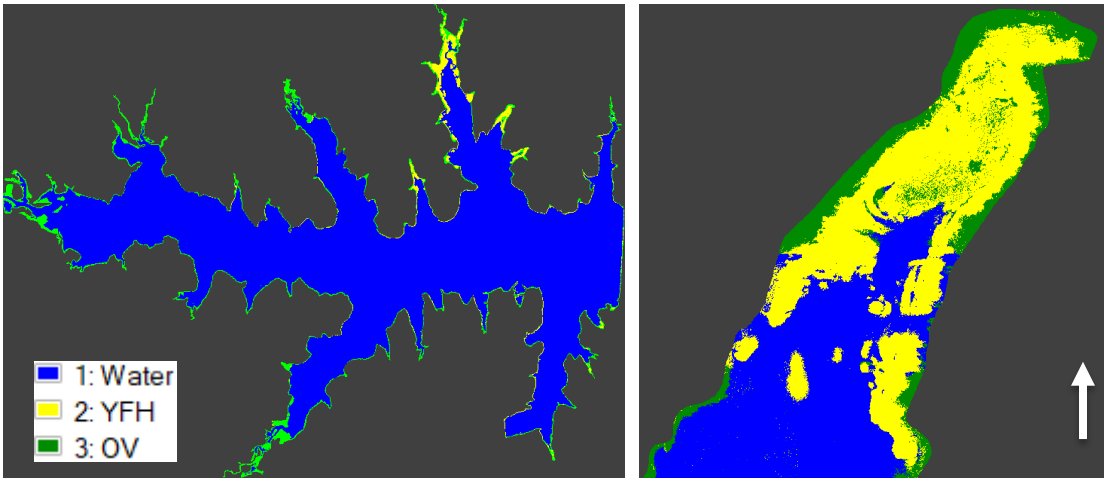

Figure 4. Left: Classified Sentinel-2 image (7-09-19). Right: Classified UAV image (7-11-19).

Reference points were created from imagery and served as reference data for the MLC accuracy assessments. A confusion matrix compared the reference data to the classification outputs for every class. Statistical parameters calculated from the confusion matrix are the Overall Accuracy (OA),the Kappa Coefficient Producer's Accuracy (PA) and User's Accuracy (UA). The OA is the percentage of pixels from all classes that were classified correctly. The Kappa Coefficient is the measurement of how well classified pixel values agree with values from reference classes, if the map were created using random classification. The PA is the accuracy of how well features in the map are correctly classified by the maker. The UA is the probability that a classified pixel represents the actual feature in the field (Harris Geospatial, 2019). This study

compares the outcomes from each sensor to classify *N. peltata*. The number of pixels classified can estimate the spatial coverage of the plant, which can be compared to hand-digitized extents.

Spatial Extent Over Time

The *N. peltata* infestation was hand-digitized in ArcMap v 10.6.1 (ESRI, Redlands, CA) to view the changes of spatial extent. This was carried out in order to: (1) understand the population dynamics lake wide for immediate management purposes, and (2) compare the extent to that estimated from the MLC because it can be more accurate than computer-based classification. This approach is useful for environmental managers until automatic classification of images can be improved for this species. All available data from the Sentinel-2 satellite and the UAV (Table 2) were digitized. Sentinel-2 covers the entire extent of the lake and allows the quantification of the entire infestation. The UAV was only flown over area Cove D to document the effects of herbicide application. The plant was distinguishable in the images based on its unique physiology, large extent, and first-hand knowledge of the spatial analyst.

4/20/19

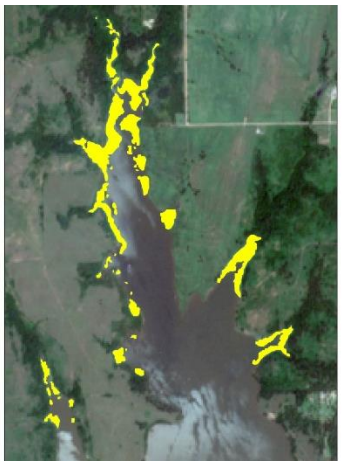

6/29/19

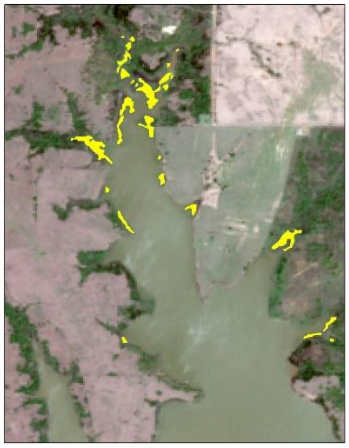

7/29/19

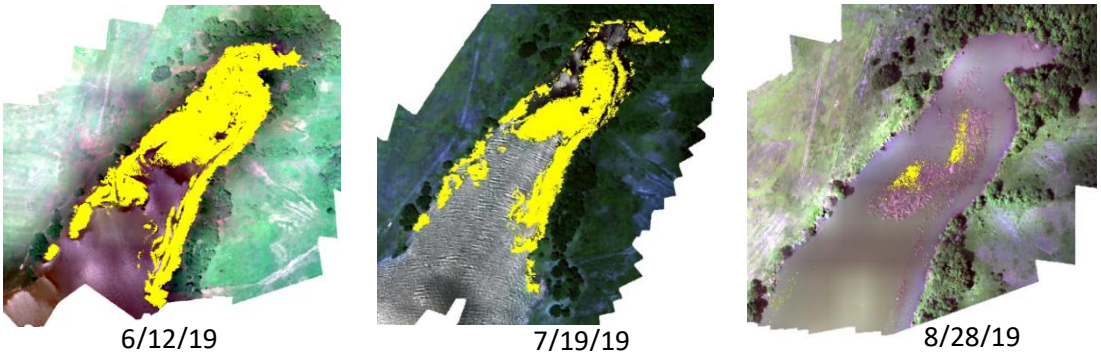

Figure 5. *Nymphoides peltata* (yellow) hand digitized in ArcGIS. Top: Close-ups of where the majority of the infestation is located. Date (4-20-19) is the earliest image where *N. peltata* is visible. Date (6-29-19) was the peak coverage date and 10 days prior to herbicide treatment. Date (7-29-19) is the infestation 20 days post-application. Bottom row: UAV imagery of study area Cove D. The high spatial resolution allows for precise estimations of plant area.

Multitemporal NDVI

The satellite and UAV imagery underwent the same workflow post pre-processing (Figure 3) to determine the NDVI and FVC values of the *N. peltata* infestation. This study calculated the following indices in Esri's ArcMap: (1) Calculate the NDVI; (2) Clip the NDVI with a shapefile to the lake extent, terrestrial vegetation; (3) Use the NDVI of the lake area to calculate FVC; (4) Extract the NDVI and FVC using peak coverage spatial extent.

It is standard to use Band 8 (NIR) and Band 4 (Red) (Table 1) to calculate the NDVI (Equation 1) for Sentinel-2. Bands 4 (NIR) and 3 (Red) were used (Table 2) to calculate NDVI for the UAV data. NDVI (Equation 1) was calculated for every pixel in an image and was given a value (-1 to 1). Pixels with values less than zero were associated with soils and non-vegetation (Jackson et al., 1983).

All imagery was clipped to the extent of the hydrologic boundary of Lake Carl Blackwell to maintain the equal extent of observation for all calculations. Pixels were selected and ArcMap was used to determine average value, standard deviation, minimum, and maximum. The peak spatial coverage of *N. peltata* was used to extract corresponding values to observe the change of vegetation response over time. Analysis values from the infestation for Sentinel-2 and UAV were

extracted for each available date and compared with linear regression to determine if there were significant relationships between the measurements of the sensors.

Normalized Difference Vegetation Index:

$$NDVI = (NIR - Red) / (NIR + Red) \quad \text{(Equation 1)}$$

The extent of *N. peltata* was then clipped from the terrestrial area and spectral values extracted using the coverage of the peak extent to measure the change over time. The FVC (Equation 2) (Song et al., 2017) uses the isolated NDVI values of *N. peltata* to estimate what percent, or density, of each pixel represents vegetation. It is calculated as:

Fractional Vegetation Coverage:

$$FVC = [(NDVI - NDVI_{min}) / (NDVI_{min} - NDVI_{max})] * 100 \quad \text{(Equation 2)}$$

where NDVI is the Index; $NDVI_{min}$ is the lowest calculated pixel value, indicating low or no vegetation; $NDVI_{max}$ is the highest calculated pixel value, indicating full vegetation cover. The index is multiplied by 100 to give a percent coverage value.

Field Validation

Field measurements were collected at Lake Carl Blackwell in 2018 that estimated the plant coverage on 2 m^2 quadrats at various locations in the infestation. These points were organized in a grid to collect points approximately 20 m apart in order to prevent spatial autocorrelation. Quadrat coverages (FVC_{ground}) were correlated to FVC calculated for Sentinel-2 imagery($FVC_{Sentinel-2}$) from 2018. It was also correlated to FVC calculated for RGB UAV imagery (FVC_{UAV}) collected in the summer of 2018 from a previous study (Angle, 2019). The satellite imagery underwent the same processing procedures as the 2019 dataset. The RGB UAV data was collected with a DJI Phantom4 drone and an off-the-shelf camera (~1 cm spatial resolution). It

was necessary to first approximate the Visible Atmospherically Corrected Index (Equation 3) prior to calculating the FVC, since this UAV dataset lacks an NIR band.

Visible Atmospherically Corrected Index (Gitelson, 2002):

$$VARI = (Green - Red) / (Green + Red - Green) \quad \text{(Equation 3)}$$

Field observations were imported to ArcMap and then buffered to a 10 m zone. The corresponding image data was extracted using the Zonal Statistics Tool. Available ground data was correlated to the 2018 $FVC_{Sentinel\text{-}2}$ data for 198 observation pairs on 10 dates (7-19-18; 7-29-18; 8-3-18; 8-28-18; 9-22-18; 9-27-18; 10-22-18; 10-27-18). The 2018 FVC_{UAV} for two dates (7-31-18; 8-9-18) were correlated to 45 ground points. Figure 6 illustrates the sampling pattern used in coves with UAV imagery and satellite imagery.

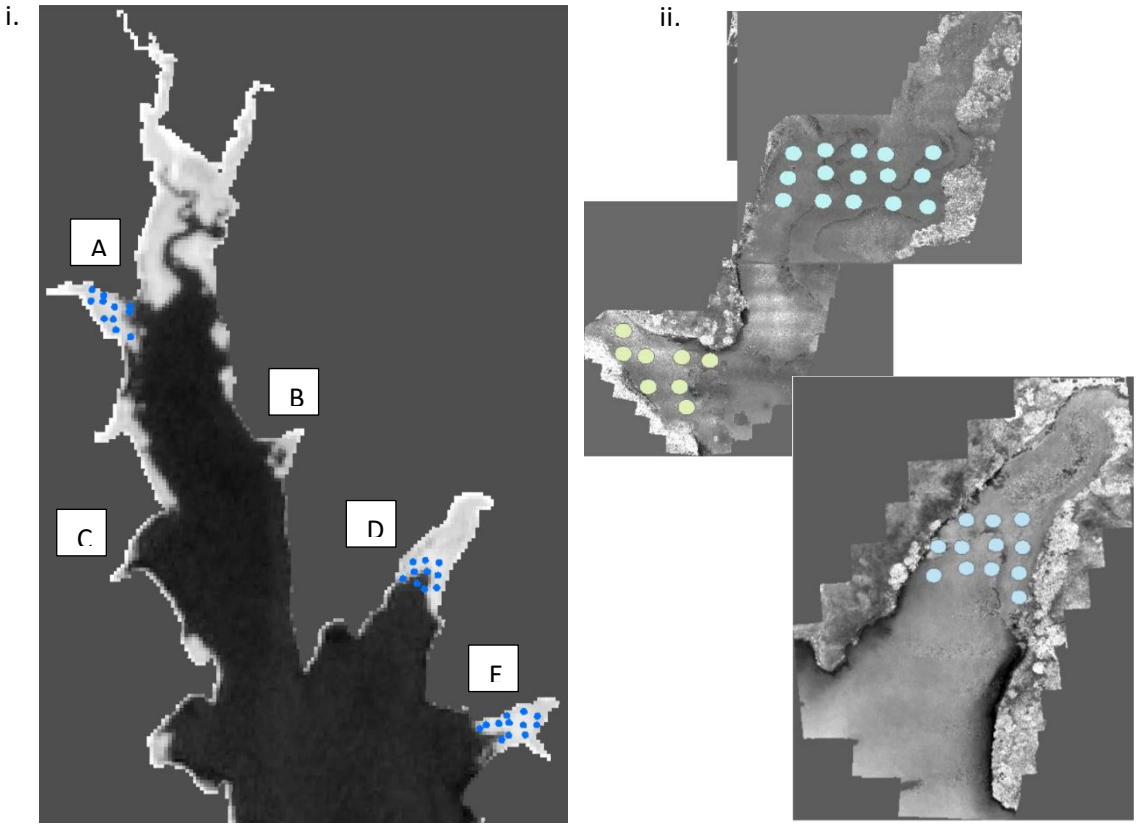

Figure 6. i. $FVC_{Sentinel\text{-}2}$ (8-3-18) with field observation points buffered to 10m overlain for zonal statistics extraction. ii: FVC_{UAV} imagery (Top, 8-9-18) (Bottom, 7-31-18) with field observation points to a 10m buffer overlain for zonal statistics.

Statistical Analysis

Linear regression is a statistical method that estimates the conditional response relationship between datasets (Seber & Lee, 2012). This study determined if there was a linear relationship between the satellite and UAV imagery for different parameters (spatial extent, NDVI values, FVC). Basic statistical values selected from Cove D were used to model a linear regression to infer the strength of the relationship between sensor spectral resolution. Linear regressions were conducted using Microsoft Excel for a dataset of seven temporally overlapping dates of satellite and UAV imagery over Cove D (Table 2), as well as ground coverage to the $FVC_{Setinel\text{-}2}$ and the FVC_{UAV}.

The classification results from Sentinel-2 and UAV imagery cannot be directly compared to each other due to significant differences of area covered by each. The area of *N. peltata* reported from the MLC step was then compared to manually derived spatial extent of the corresponding sensor using regression analysis. This indicates if classification accuracy is comparable to manual classification and if it is valuable in vegetation monitoring.

Economic Analysis

The costs of sensors and the analysis of the imagery are an important aspect to consider. Satellite imagery of very high resolution or targeted return time can be more expensive than what is reasonable for most environmental projects. The costs of UAV and cameras are also very expensive though they offer flexible data collection on demand. This study considers the costs of equipment in addition to treatment and administrative costs associated with the project. Management at Lake Carl Blackwell has tried in the past to control the *N. peltata* infestation with little success. A review of costs from 2018 and 2019 were analyzed to estimate the costs per hectare of treatment for both years.

The value of the lake area as a whole can be deduced from the revenue generated. LCB is a popular recreation area that is open for boating and fishing year-round and generates revenue through the sale of: annual permits, nightly camping, daily permits, equestrian usage, and leased sites. Accounting of the monthly revenue was provided by LCB management and analyzed in Microsoft Excel for the months of April to October 2019. The average monthly revenue was calculated and used as a benchmark to estimate the Monthly Lake Value (MLV) (Equation 4).

Equation for Monthly Lake Value:

$$MLV = \Sigma \text{ Monthly Revenue of LCB} \div 7 \text{ months} \quad \text{(Equation 4)}$$

The MLV was expanded to estimate Monthly Hectare Value of LCB by dividing the MLV by the waterbody area (1,300 ha) (Equation 5). The MHV gives an approximation of how much each ha on the lake is worth in terms of recreational access.

Equation for Monthly Hectare Value:

$$MHV = MLV \div 1{,}300 \text{ ha} \quad \text{(Equation 5)}$$

The Potential Lost Value (PLV) can be estimated by multiplying this value by the number of ha of *N. peltata* that are present. The average ha value was selected for this calculation for each month. The PLV is essentially the lost value of the lake as an impact from the spatial extent of *N. peltata* over time (Equation 6):

Equation for Potential Lost Value:

$$PLV = MHV \times \text{ha of } \textit{N. peltata} \quad \text{(Equation 6)}$$

CHAPTER IV

RESULTS

Image Classification and Accuracy Assessment

Sixteen images from Sentinel-2 were classified to an extent of approximately 9x12 km. Three classes (Figure 4) were produced from the Maximum Likelihood Classification (MLC) and the parameters OA, Kappa Coefficient, PA, and UA were generated for the *N. peltata* vegetation class (Figure 7). The OA ranged from 75.5% to 100%, which equated to an average of 96.1%. One of these dates had an OA of 75.5% and the rest were greater than 92%. Reported Kappa Coefficients were 0.27 to 1.0. The lowest coefficient value corresponds to the lowest OA on 10-27-19 (DOY 300). The PA (50 – 100%) and UA (22.7 – 100%) reflect the confusion matrix results of *N. peltata* vegetation class as compared to the reference data. The ratio of reference to training pixels for *N. peltata* of this dataset was 7 – 36%. Lower UA values occurred with fewer training pixels, which is a result of the herbicide treatment (Table 4).

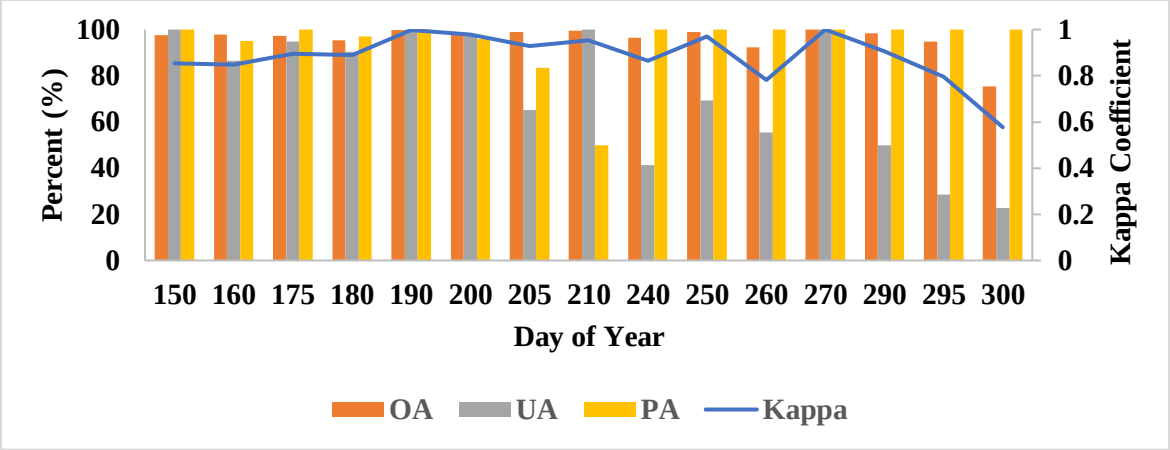

Figure 7. Sentinel-2 classification accuracy assessment results. The X- axis is the Day of Year for each date, a measurement that gives the absolute day of the year. The orange bars indicate the overall accuracy, gold bars represent the Producer's Accuracy, and the User's Accuracy is marked with gray bars. The Kappa Coefficient is the blue line that aligns to the secondary horizontal axis.

MLC classified *N. peltata* from Sentinel-2 imagery an average 95% of the time. The ratio of reference to training pixel was 7 to 37% on average. The number of pixels available was greatly diminished contributing to poorer classification, as the infestation declined over time.

Table 4. Sentinel-2 *N. peltata* training and reference data.

Day of Year	Date	Training Pixels #	Reference Pixels #	Ratio
150	5/30/2019	708	53	0.07
160	6/9/2019	338	40	0.12
175	6/24/2019	485	111	0.23
180	6/29/2019	408	97	0.24
190	7/9/2019	571	116	0.20
200	7/19/2019	235	50	0.21
205	7/24/2019	49	18	0.37
210	7/29/2019	20	4	0.20
240	8/28/2019	22	7	0.32
250	9/7/2019	44	9	0.20
260	9/17/2019	40	10	0.25
270	9/27/2019	38	7	0.18
290	10/17/2019	34	7	0.21
295	10/22/2019	17	6	0.35
300	10/27/2019	49	10	0.20

Three classes (Figure 4) were produced from the MLC of the UAV imagery dataset. The confusion matrix resulted in OA 88.3 to 97.8% and Kappa coefficients 0.30 – 0.95. The PA of *N.*

peltata ranged from 70.70 to 99.99% and UA was 15.95 – 97.91% and averaged 70.21% (Figure 8).

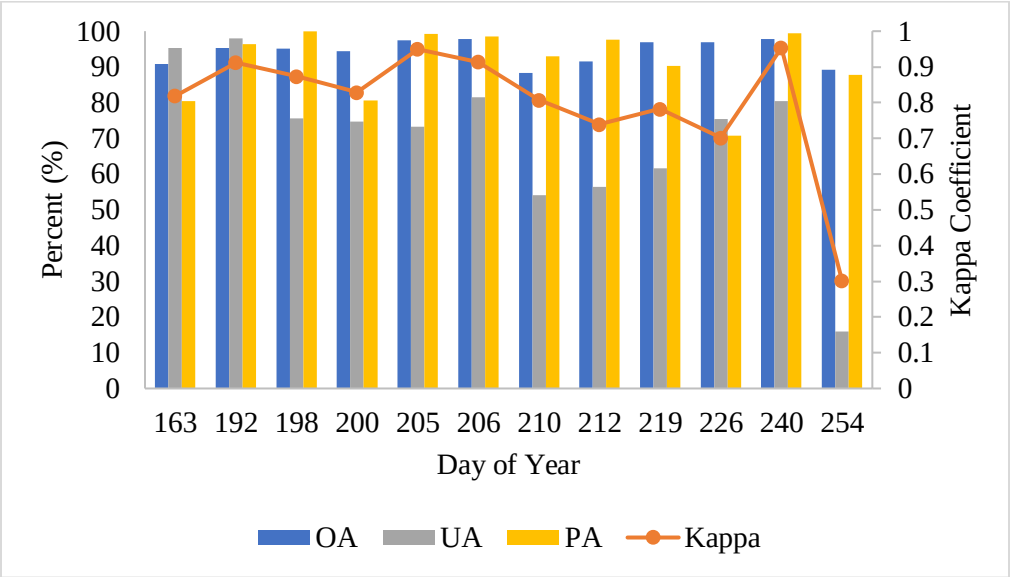

Figure 8. Accuracy assessment of UAV images from summer 2019. The Overall Accuracy are represented by the blue bars, Producer's Accuracy are the gold bars, and the User's Accuracy denoted by the grey bars. Kappa Coefficient is the red line and is scaled to the secondary horizontal axis.

Low UA could be attributed to declining vegetation reflectance as it becomes more stressed. The training to reference pixel ratio ranged from 0.18 to 0.56. The average without the outlier is 0.22 and with it is 0.28 (Table 5).

Table 5. Accuracy Assessment of *N. peltata* in 2019 UAV imagery.

Day of Year	Date	Training Pixels #	Reference Pixels #	Ratio
163	6/12/2019	145,354	35,120	0.24
192	7/11/2019	387,562	217,906	0.56
198	7/17/2019	93,983	20,785	0.22
200	7/19/2019	155,287	31,045	0.20
205	7/24/2019	49,014	9,010	0.18
206	7/25/2019	67,995	14,311	0.21
210	7/29/2019	33,781	7,235	0.21
212	7/31/2019	160,539	35,832	0.22
219	8/7/2019	33,652	9,783	0.29
226	8/14/2019	31,213	6,671	0.21

240	8/28/2019	32,336	8,195	0.25
254	9/11/2019	12,327	2,618	0.21

Spatial Coverage

The spatial extent of *N. peltata* was estimated and compared using Sentinel-2 and UAV imagery. The wide area covered by Sentinel-2 made it possible to estimate the infestation lake wide. The smallest detectable area of *N. peltata* with Sentinel-2 was 0.01 acres. Sentinel-2 images showed that *N. peltata* surfaced in April at approximately 6.52 ha and peaked around 22.5 ha in July 2019 (Figure 9). There was an approximate 91% reduction in coverage within 15 days after treatment on July 9. *Nymphoides peltata* declined for 56 days to less than 0.85 ha in the final image on 10-27-19.

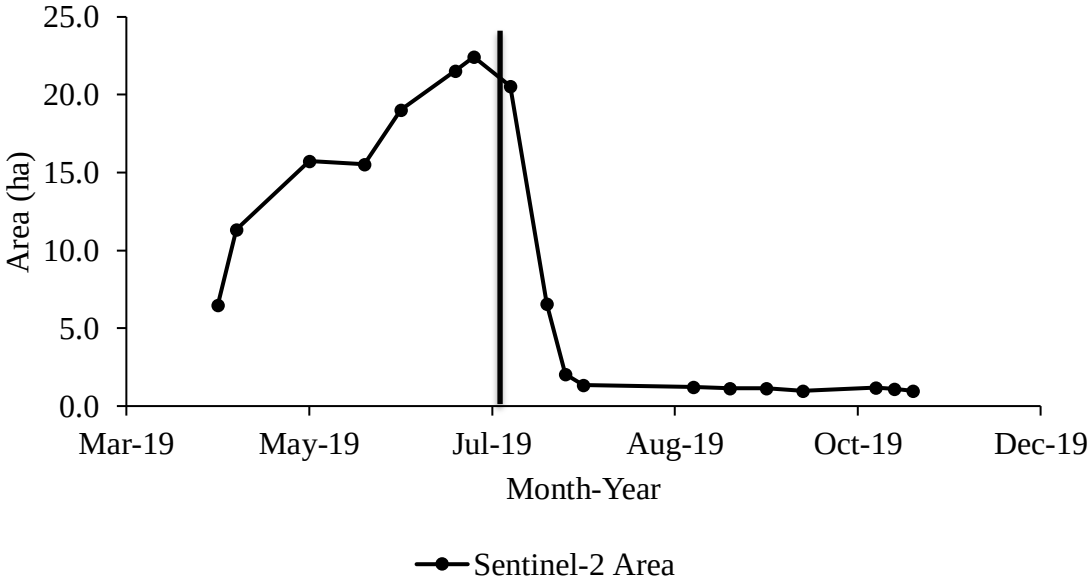

Figure 9. Lake wide spatial coverage of *N. peltata* over the summer of 2019 derived from Sentinel-2 satellite imagery. The black line represents the first day of herbicide treatment.

Coverage of *N. peltata* in Cove D measured with Sentinel-2 exhibited a similar declining trend as the lake wide infestation and peak coverage in this area was estimated at 2.98 ha (Figure 10). UAV imagery yielded similar estimates of *N. peltata* coverage in Cove D as Sentinel-2. There was an increase from 2.09 ha in June to a peak of 2.59 ha in July. UAV data captured a

77% decline in the study area 15 days after treatment. The final date of the UAV dataset estimated a coverage of 0.03 ha. The exact area of the hydrologic boundary used in the GIS analysis was 1313 ha. It is shown that *N. peltata* grew to almost 2% of the lake's surface area from the lake geometry and the area of the vegetation coverage over time. The efficacy of ProcellaCOR reduced that coverage from 1.71% to 0.16% in 20 days. The area remains consistent until over wintering.

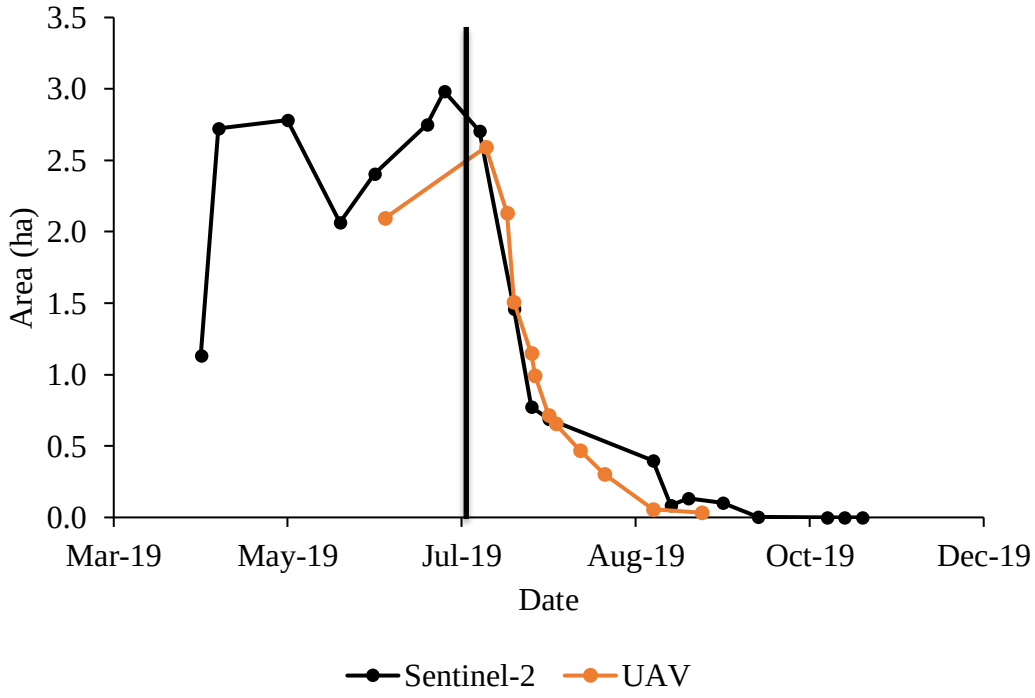

Figure 10. Spatial coverage of *N. peltata* over the summer of 2019 in the study location Cove D taken with Sentinel-2 (black) and UAV (orange). The black line represents the first day of herbicide treatment.

Regression analysis was used to compare coverage estimates between platforms for seven temporally corresponding dates (Table 3). Results showed a significantly high positive relationship ($R^2 = 0.94$; $p < 0.001$) between datasets from the two sensors to visually delineate the infestation (Figure 6). The classified data can be further validated by comparing the spatial area tabulated for *N. peltata* from the MLC with regression analysis. Table 6 summarizes the comparison of the hand digitized coverages from UAV (UAV_{Dig}) and Sentinel-2 ($S\text{-}2_{Dig}$) to the

classified data (UAV_{class}; $S\text{-}2_{class}$) of its respective sensor. The Sentinel-2 data (n = 16) had a low positive relationship ($R^2 = 0.11$) that was not significant at $p = 0.23$. The multispectral UAV data (n =11) had a significant positive relationship ($R^2 = 0.87$; $p < 0.001$).

Table 6. Regression analysis results from the comparison of the hand digitized coverages UAV (UAV_{Dig}) and Sentinel-2 ($S\text{-}2_{Dig}$) to the classified data (UAV_{class}; $S\text{-}2_{class}$) of its respective sensor.

	N pairs	R^2	Significant *f*	Standard Error
UAV_{Dign} : $S\text{-}2_{Dig}$	7	0.94	< 0.001	0.26
$S\text{-}2_{Dig}$: $S\text{-}2_{class}$	16	0.11	0.23	24
UAV_{Dig} : UAV_{class}	11	0.87	< 0.001	0.29

Normalized Difference Vegetation Index

The lake wide average NDVI of *N. peltata* was 0.09 in the first available Sentinel-2 image on April 20, 2019. Maximum average NDVI values were 0.60 in June and the minimum average NDVI value was -0.21 in late October. The lake wide average NDVI value gradually increased to 0.60 prior to the herbicide treatment (July 9, 2019) after which it declined rapidly (Figure 11).

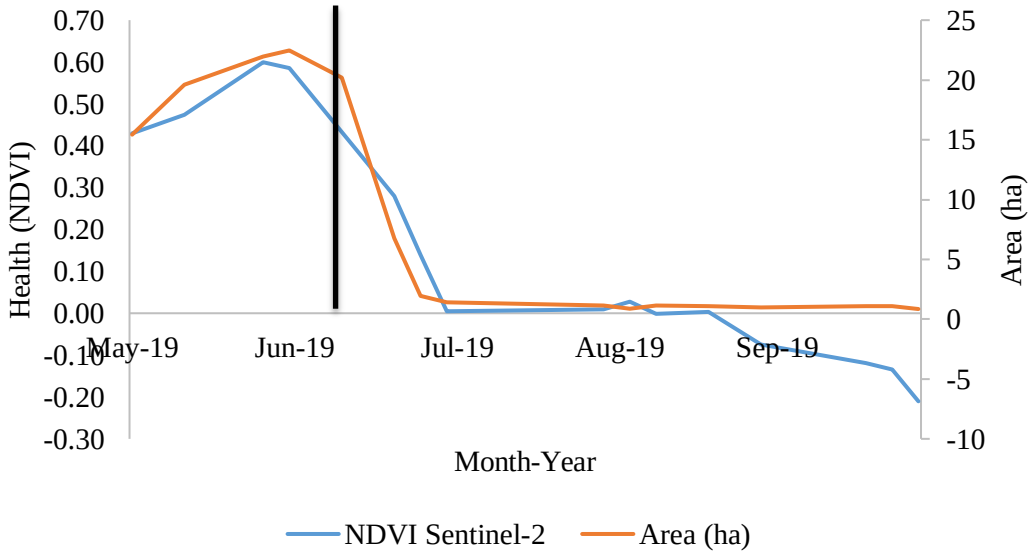

Figure 11. Spatial coverage (blue line) and average NDVI (orange line) values for *N. peltata* over the summer of 2019 lake wide, derived from Sentinel-2 imagery. The black line indicates the day of treatment.

The average NDVI values from Sentinel-2 imagery for Cove D peaked at 0.62 in July and declined to 0.07 (Figure 12). Values derived from UAV imagery for Cove D (Figure 12) peaked at an average of 0.42 in July and declined for 9 weeks post-treatment to a low of -0.15. Values from both sensors had sharp declines soon after herbicide treatment and reinforces the visual estimate of efficacy.

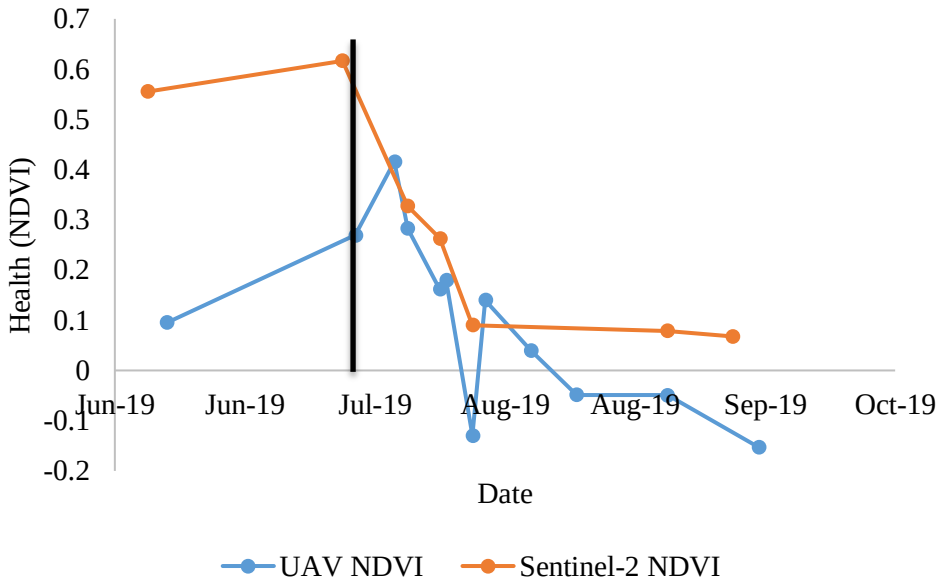

Figure 12. NDVI of *N. peltata* over the summer of 2019 in the study location Cove D, derived from Sentinel-2 (orange) and UAV (blue) imagery.

Seven dates (Table 3) from Sentinel-2 and UAV were used to compare NDVI data using linear regression. Results showed a positive relationship ($R^2 = 0.40$) between the two sensor's spectral measurements, but this relationship was not significant ($p > 0.05$). They both exhibited a sharp decline that would indicate that the vegetation was becoming stressed and eventually being replaced by water pixels, which have negative NDVI values. The UAV shows a more dramatic decline of NDVI that could be attributed to its greater spatial resolution.

Fractional Vegetative Cover

Emergent coverage of the lake wide $FVC_{Sentinel-2}$ averaged 76.2% on April 20, 2019. Peak average FVC was 82.3% July 9, 2019 and dropped to a low of 33.6% about 11 weeks after treatment (Figure 13). Sentinel-2 data from the study area Cove D showed a maximum FVC of 62% in July, which was the day of treatment. It then had a minimum reported average of 38% 20 days later (July 29, 2019).

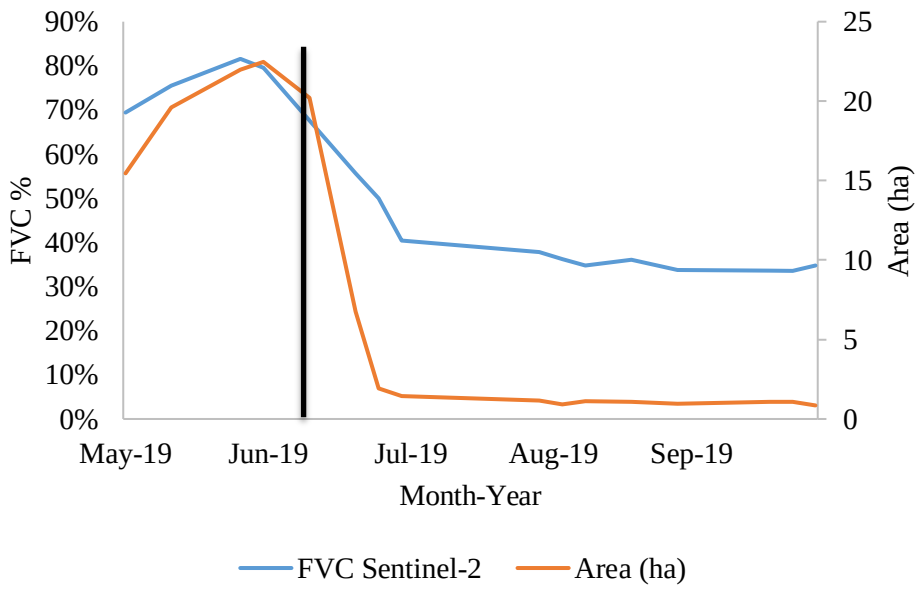

Figure 13. Fractional cover (orange) and spatial coverage (blue) of *N. peltata* over the summer of 2019 in the study location Cove D, derived from Sentinel-2 and UAV imagery.

The FVC_{UAV} pixel average peaked at 71% (July 17, 2019) and had a low of 42% in September (Figure 14). The standard deviation ranged from 4.3 to 33.3%. The regression analysis of the FVC datasets had seven observation pairs (Table 2). The data had a positive relationship ($R^2 = 0.39$), but the relationship was not significant ($p > 0.05$). The low significance is impacted by the low sampling size of the dataset and could be improved with more frequent data collection. Calculation of the FVC allowed comparison of ground quadrat measurements to UAV and Sentinel-2 pixel values.

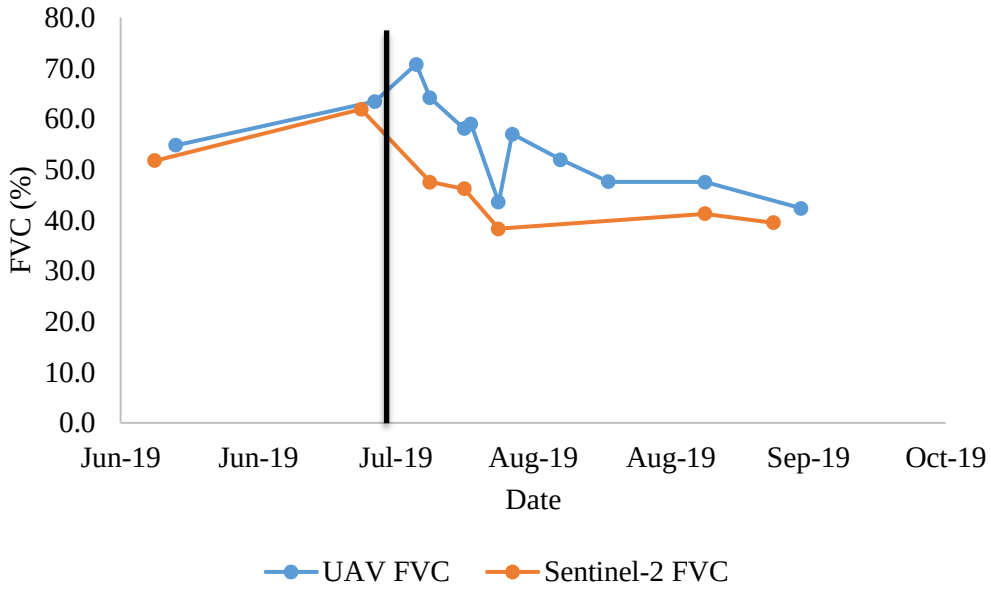

Figure 14. Fractional cover of *N. peltata* over the summer of 2019 in the study location Cove D, derived from Sentinel-2 (orange) and UAV (blue) imagery.

Field Validation

Ground measurements collected in 2018 were analyzed along with FVC data derived from Sentinel-2 and RGB UAV imagery collected over the summer of 2018. Ground measurements were buffered to 10m to correspond with the pixel size of Sentinel-2. Satellite data from 10 dates was analyzed to obtain 198 validation pairs. The UAV imagery dataset had only two days of imagery appropriate for correlation to ground cover (n = 45 pairs) (Table 7)

The Sentinel-2 average FVC ranged from 16 to 98% for an overall mean of 47%. The field measurements averaged 61% in the corresponding areas. A significantly positive relationship was observed between FVC_{ground} and $FVC_{Sentinel\text{-}2}$ ($R^2 = 0.47$; $p < 0.001$). The mean FVC_{UAV} ranged from 15 to 62% for an average of 37.15% as well. There was not a significant relationship between FVC_{ground} and the UAV points ($R^2 = 0$; $p > 0.05$) likely due to pixel scale differences. The field measurements do show there is validation of the presence/absence of vegetation at each point.

Table 7. Regression analysis results from the comparison of the ground sampling (2018) to UAV (RGB, 2018) and Sentinel-2 .

	N Pairs	Sensor FVC range	Mean FVC	SD FVC Sensor	Ground FVC	Mean FVC	R^2	SE	*P*
Ground v Sentinel-2	198	16 - 98%	47%	18%	0 - 100%	61%	0.47	13	< 0.001
Ground v UAV	45	19 - 52%	47%	15%	0 - 100%	62%	0.01	15.2	> 0.05

Economic Analysis

Monitoring costs for this project varied for each sensor. The Sentinel-2 satellite is an open-access platform. The imagery and processing software are available for free from ESA. Processing and analysis of this imagery requires a trained analyst knowledgeable about the infestation, which could be costly. The UAV imagery had a much higher startup cost than Sentinel-2 data. Angle (2019) estimated image analysis to be about $100 per image for either platform, the UAV equipment and software totaled around $13,500 (Table 8).

Table 8. Summary of the costs of equipment and analysis for the Sentinel-2 and UAV imagery.

	UAV	**Sentinel-2**
Camera/Drone	$8,800	$0
Software	$3,500	$0
Analysis	$1,200	$1,800
Total	$13,500	$1,800

Project costs included more than just the monitoring equipment (Table 9). The herbicide required to treat all ~20 ha of *N. peltata* cost $19,000. Equipment and labor for the herbicide application in 2019 was over $35,000 and included a third-party applicator as well as costs for an airboat operator from the Oklahoma Department of Wildlife Conservation. Costs for a calibrated herbicide sprayer were $5,500. Water samples were collected and analyzed in order to determine the product was not reaching the water intake of the reservoir. All samples were found to be below detection limits. Administrative costs totaled over $37,000. The total project costs were

approximately $106,000. Oklahoma State University at this time chose to switch their water source from Lake Carl Blackwell to the city supply, however, these costs were not able to be factored in for this study.

The spatial analysis revealed that approximately 91% of the infestation was controlled in an 8-week timeframe. This is what SePro predicted would happen post-application. This equates to about $5,200 per ha of control. This is in contrast to control efforts exerted in 2018. Glyphosate was applied as a treatment in 2018 but only successfully controlled about 1 ha of *N. peltata*. The monitoring costs were less than what was used in 2019 because it used an off-the-shelf camera rather than the multispectral MicaSense RedEdge camera that costs around $5,500. The 2018 project costs were around $66,000. This is approximately 62% less than the 2019 project costs. The 2018 glyphosate application yielded almost no control and cost about $66,000 per ha of *N. peltata* eradication.

Table 9. Summary of the Project costs at Lake Carl Blackwell in 2018 and 2019.

	ProcellaCOR	**Glyphosate**
Application Labor/ Equipment	$35,007	$6,200
Monitoring/Analysis	$13,500	$7,960
Water Tests	$800	$6,960
Administrative	$37,347	$43,200
Product	$19,000	$1,950
Total	$105,654	$66,270
$/ha Control	$5,283	$66,270

Lake revenue was accounted for April – October 2019 (Table 10) and includes all income from daily use permits, annual permits, cabin leases, camping sites, and store sales. *Nymphoides peltata* was present for at least 214 days in 2019, as visible from Sentinel-2 data. Lake revenue totaled just below $744,000. The Monthly Lake Value (MLV) averaged $106,283 in 2019. Corresponding MHV averaged about $82. Potential lost value ranged from $82 to $1,745, averaging a PLV of $662 per month.

Table 10. Summary of monthly revenue from Lake Carl Blackwell from April to October 2019. Monthly Revenue is the sum of all income to LCB. MLV is the average of revenue for each month. The MLV values are divided by the lake area (1,300 ha) to determine the MHV. The MHV is multiplied by the average *N. peltata* coverage from each month as measured by Sentinel-2 satellite imagery.

	April	**May**	**June**	**July**	**August**	**September**	**October**
Monthly Revenue	$69,348	$123,214	$157,377	$133,875	$104,894	$78,902	$76,373
MLV ($)	$106,283	$106,283	$106,283	$106,283	$106,283	$106,283	$106,283
MHV ($)	$82	$82	$82	$82	$82	$82	$82
N. peltata (ha)	9	16	21	8	1	1	1
PLV ($)	$731	$1,276	$1,745	$619	$94	$84	$82

CHAPTER V

DISCUSSION

The goal of this study was to investigate how data from the Sentinel-2 satellite compared to data collected with a UAV equipped with a multispectral camera for the purpose of monitoring aquatic plants. Environmental projects are often restrained by budgets and manpower that the integration of a remote sensing platform could lessen. Both platforms have positive aspects that make them feasible for vegetation monitoring, as well as significant drawbacks.

Sentinel-2 is limited by weather and poor atmospheric conditions. Imagery may not be available as it is needed for this reason. It is an open-source platform with good resolution and is relatively simple to work with by an analyst. UAV are useful for on-demand data collection with high spatial resolution and access to hard to reach areas. They are limited by their flight range, high startup costs, and technical requirements. Direct comparison of the classification results, spatial coverage, NDVI, and FVC between these two platforms have not been carried out to date. Making direct comparisons between these two platforms was intended to demonstrate if these instruments were suited for aquatic plant monitoring and its response to chemical treatment.

The overall accuracy of the 16 Sentinel-2 images was 96.1% and a Kappa Coefficient average of 0.88. Maximum Likelihood Classification of three spectral classes and four spectral channels yielded PA of *N. peltata* in this study from 50 to 100%. All imagery dates had a PA greater than 90% except the final image which had a value of 50% and one other date had PA of 75% . This is comparable to Villa et al (2015) who achieved an OA of 90.41% on four

macrophyte community images with medium resolution satellites (10 – 30 m; 400 – 900 nm). Faidi, Hasan, and Shamasuddin (2018) also used Sentinel-2 to identify *Nelumbo nucifera* using Maximum Likelihood with accuracy results of 89%.

The UA values were fairly consistent, but there was a notable decline of values after treatment with the lowest value of 22.7%. This would indicate low probability that the classified pixel would actually be found on the ground. Imagery was selected for adequate atmospheric conditions, but there were days that exhibited darker atmospheres, possibly because of the timing of image acquisition by Sentinel-2. This could have inhibited the spectral resolution to make the classification. It could have been due to reduced coverage of *N. peltata* for fewer training and validation pixels, as well as the increased stress of the plant after treatment.

The overall accuracy of the 12 UAV images was 94.3% with an average Kappa coefficient of 0.79. The UAV dataset in this study showed PA range from 50 – 100% and UA from 16 – 100%. Every date produced UA greater than 54%, except the final date. This is likely due to the very low vegetation coverage and high stress caused by the herbicide treatment. These results are similar to Husson, Hagner, and Ecke (2014) who classified vegetation in a lake environment with a UAV (OA = 95.1%).

The classification results between the two sensors were comparable, even though the UAV imagery has much higher spatial resolution and was classified using five bands that included the NIR and the Red Edge. The Sentinel-2 imagery has 10m resolution and utilized only the Red, Green, Blue, and NIR bands. Processing of UAV data took on average 2.5 to 3 hours for each image. Processing Sentinel-2 data took about 1.5 to 2 hours to classify and assess for accuracy. The high spatial resolution and relatively small classification area make the UAV dataset slightly more accurate for classification than Sentinel-2.

Regression analysis of the visual coverage estimates of *N. peltata* from the two datasets revealed a significant relationship ($R^2 = 0.94$; $p < 0.001$). This suggests that the Sentinel-2 MSI has meaningful ability to detect vegetation features at low levels. A trained analyst would be able to visually estimate the extent of the vegetation at a level that is comparable to a high-resolution UAV. This means the declining trend of lake wide *N. peltata* (Figure 8) is reliable and can be used to monitor vegetation change. This measurement estimated that the lake coverage of this plant declined from almost 2% to less 0.2% due to the application of ProcellaCOR.

The UAV imagery over Cove D allowed for precise measurements of the infestation and let the digitizer take into account open-water patches or to exclude vegetation and other features that were not *N. peltata*. The primary difference between these spatial estimates are the time requirements to digitize an image (Sentinel-2 ~ 30 minutes; UAV ~ 3 hours). *Nymphoides peltata* was identifiable at a spatial extent of about 40 m^2 and so for a vegetation stand less than this the UAV would be able to provide more reliable coverage than what is gathered from the UAV.

Results of this analysis also provide support for the herbicide manufacturer's claim to reduce weed species in 6 – 8 weeks. The satellite imagery documented a 91% reduction in just 15 days. A similar trend was observed by the UAV in Cove D with a 77% reduction in 15 days. Willey & Langeland (2018) achieved partial control of *Nymphoides cristata* with glyphosate and imazapyr with some success, but the plant regenerated in just four weeks. The Oregon Department of Agriculture achieved 95% reduction of an *N. peltata* population at Umpqua National Forest using Imazapyr (ODA, 2018). This suggests ProcellaCOR may be more successful than similar herbicides like glyphosate or imazapyr. The extreme reproductive potential of *N. peltata* to reproduce from fragments and propagules make physical removal impractical and ProcellaCOR would be a better alternative.

The spatial extent of *N. peltata* produced from the MLC were as much as three times greater than the area manually digitized for Sentinel-2. The regression analysis showed a weak relationship that was not significant ($R^2 = 0.11$; $p > 0.05$). Classification to detect and delineate infestations would need to be greatly improved for this sensor in order to be reliable. Sentinel-2 tended to overestimate the spatial extent of *N. peltata.* The hand digitized spatial extent from Sentinel-2 had a significantly close relationship to the values that were derived with the UAV. It could be used to reliably estimate *N. peltata* over a large area by an analyst familiar with the plant and the study area if it covered a sufficient spatial extent.

The area derived from the classification of UAV imagery had a closer relationship to the digitized area than was seen with the 10 m satellite imagery. Regressions of the classified area from UAV imagery had a high relationship ($R^2 = 0.87$; $p > 0.05$), but the results were not significant. The low significance is likely due to the small sample size of the dataset and would require a higher frequency of data collection. Maximum Likelihood Classification of UAV imagery would be useful for analyzing data collected over a new area where it was unclear if the vegetation present was *N. peltata*.

The NDVI values for both sensors dropped significantly after 25 days even though total eradication was not achieved. No regrowth was observed. The relationship between the seven chosen dates was positive though the regression indicates low significance ($R^2 = 0.40$; $p > 0.05$). This would also be due to the low sample size of the dataset. The dates that have significantly different outcomes have low light atmospheric conditions and lower levels of *N. peltata* to measure. The extracted pixel values corroborate the visual assessment that treatment resulted in a significant decline of vegetative health quickly reducing spatial coverage. Sentinel-2 was able to capture this lake wide and was supported by the targeted UAV data collection. This supports the claim of short residency time by the herbicide, even though total eradication was not achieved.

It should be noted that some areas of the infestation were inaccessible for spray application due to dense willow stands or lack of terrestrial access. The FVC was directly derived from NDVI values and therefore exhibited similar trends. $FVC_{Sentinel-2}$ measured an average peak of 82% that declined to 34% after treatment. The FVC_{UAV} imagery over Cove D peaked at 71% and declined to 42% post-treatment. The correlation between the Sentinel-2 and UAV imagery was about the same ($R^2 = 0.39$; $p > 0.05$) as the NDVI relationship. The lower relationships between sensors is likely due to differences of pixel size and sample size.

These measurements were validated by the ground measurements from the 2018 UAV and satellite datasets. The buffer size around the ground points could have been too large to adequately estimate the FVC_{UAV}. There was not a significant relationship between coverage measurements from the field to the FVC calculated for the RGB UAV imagery. This could be due to the spectral characteristics of the VARI equation and to the small pixel size. These measurements support a presence/absence correlation of vegetation at the time. Differences can be attributed to scale differences to the quadrat measurements. Results indicate the presence/absence of *N. peltata* can be confidently ascertained from Sentinel-2 imagery.

The potential lost value caused by the *N. peltata* infestation was based on assumptions that lake value could be estimated by net revenue generated by lake users in the summer months of 2019. It extends this assumption so that the physical area of the lake has a monetary value based on its availability of use. The entire lake would be accessible to patrons without the infestation. *Nymphoides peltata* grows at high densities and large spatial extent as to render some areas unusable. Multiplying the monthly ha value by the monthly average spatial extent gives the cost of the area occupied by the infestation. An estimated $4,631 of value was lost from the lake in the summer of 2019. This is not actual money lost, but it is value of the lake that has been diminished. The *N. peltata* infestation could potentially spread around the perimeter of the lake and cause a much more significant loss of value if nothing were to be done.

CHAPTER VI

CONCLUSION

New and innovative technologies are improving our ability to monitor vegetation. Remote sensing will be a primary tool for invasive plant detection and monitoring moving forward. This requires that *N. peltata* be accurately classified from the selected platforms. Sentinel-2 has a scale that required it to classify an image far larger than the extent captured by the UAV. Sentinel-2 demonstrated a tendency to over-estimate *N. peltata* than what was estimated visually. This could be overcome with more training of classifying algorithms. The UAV showed very high potential to classify *N. peltata* that was confirmed by the relation of classified area to the manually digitized area. The accuracy of results was impacted by the effects of the herbicide. The resulting user's accuracy declined after treatment in response to the limited area of *N. peltata* as what was left was highly stressed and produced varying spectral responses. UAV classification would be useful in instances where it is uncertain if an area has an *N. peltata* population. The flight flexibility and very high spatial resolution of a UAV makes it easy to target new areas with unconfirmed potential infestations. The average lake monitoring plan would likely survey areas of known vegetation and so it is unlikely they would need to enact such a complicated measure as image classification.

Sentinel-2 demonstrated high potential for manual detection of *N. peltata* in this study. It was able to quantify the seasonal trend and its decline over the entire lake. This was validated by the statistically significant positive relationship between the Sentinel-2 and the UAV derived

spatial extent. The high spatial resolution of the UAV can reliably image *N. peltata* and allowed for precise measurement. Sentinel-2 provides similar coverage estimates even though it captured data at coarser spatial scale. The Sentinel-2 images are free compared to the UAV which has expensive startup and use costs which is something for project managers to consider.

These sensors seemed to similarly demonstrate that the average NDVI values dropped suddenly after treatment. They were able to document the negative effect of ProcellaCOR on plant growth and productivity. This would suggest that both sensors provide meaningful spectral measurements and can be used to monitor herbicide treatments. The UAV should be flown over the entire infestation for better comparison to address this question. The difference of outcomes between the sensors could be attributed to the coarser spatial resolution of Sentinel-2. Few studies exist that compare the outcomes of spectral indices based on spatial resolution without re-scaling the data, so the true relationship is difficult to estimate. The importance of the outcomes of this study lie in the similarity of the trends.

Both platforms have positive aspects and limitations that may dictate how they are used in environmental projects. UAVs are generally well-suited for short-term monitoring over relatively small areas that allow for on-demand data collection. This was useful for documenting the short-term changes in the days immediately before and after herbicide treatment. A drawback of UAVs are the high costs for equipment and processing software and the substantial time needed for data collection and processing. The UAV also requires substantially greater technical knowledge to composite and use multispectral data than Sentinel-2. The hiring of a third-party for analysis could increase costs substantially and is something that should be considered by lake managers. Sentinel-2 is ideal for imaging large areas for wide scale detection and mapping.

The choice of sensor is highly dependent on project goals and data needs. The satellite platform should be a sufficient tool for monitoring trends in aquatic plant vegetation in most

cases. The UAV can be a good substitute for ground surveys but would probably be used under limited circumstances. The UAV can provide data in targeted areas on short notice. The UAV may also be advantageous if the lake manager wants to study the immediate effects of treatment that cannot be documented in the 5-day overpass schedule of Sentinel-2. The UAV is still limited by weather conditions but can still collect meaningful data in overcast conditions that would occlude the ground from the satellite platform.

The success of ProcellaCOR to reduce the extent and health of *N. peltata* was easily captured to the full extent using the satellite imagery. It would be most practical and cost-effective to use the Sentinel-2 MSI imagery to delineate biological vegetation parameters prior to and over the course of treatment over a large scale. This would indicate the general response and the short temporal resolution make it ideal for seasonal monitoring. The UAV provides more data in specific areas that the Sentinel-2 MSI cannot capture. The Sentinel-2 platform should be used until the vegetation reaches such low densities and area as to not be identifiable at this scale. The UAV would be more appropriate in this case. The high costs and technical knowledge make the UAV less usable in an average vegetation monitoring project. The costs would need to be considered along with how often the manager thinks it would be used before the investment is made. The UAV platform may be best suited for scouting new areas that are unreachable or if there is a presence of overhanging canopy. It is also well suited for monitoring where the vegetation covers such a small area that the satellite does not indicate the presence of vegetation.

The SePRO corporation that produces and sells the herbicide ProcellaCOR claims full eradication of invasive weeds within 6 – 8 weeks. It has only been on the market for about two years at the time of publication and primarily used to treat small ponds. Its use at Lake Carl Blackwell is one of the first applications at a large scale and in an open waterbody. The satellite data indicate that the infestation was reduced by 91% in this 8-week time frame. Full eradication

was not achieved, but the results indicate that this herbicide is extremely effective at least seasonally.

Areas that were not affected did not have the herbicide directly applied due to lack of access. This is consistent with the other claim SePRO makes about the herbicide having low-residence time in water and does not travel. This is corroborated by the water testing that showed no detectable limits of ProcellaCOR at the water intake. It is presently unclear what the effects will be in the long term and how much regrowth can be expected in an environment such as Lake Carl Blackwell.

The product costs of ProcellaCOR were considerably higher than the glyphosate the lake had used in the past. Project costs for 2019 were estimated to be approximately $106,000. This is about 60% higher than project costs in 2018 when glyphosate and hand removal were the treatment methods. ProcellaCOR exerted considerably better vegetation control than glyphosate despite the difference in overall project costs. ProcellaCOR demonstrated a cost of about $5,300/ha whereas glyphosate cost about $66,000/ha of control.

A lake manager would be prudent to use a combination of these sensors to maximize their data collection. The Sentinel-2 satellite would be a cost-effective method to monitor seasonal change when vegetation is of a high enough spatial extent. It has the added advantage of imaging a very large area providing large amounts of data for analysis. The UAV does not have the capacity to image as large an area as the satellite and would require the coordination of multiple drones. This would magnify the costs associated with UAV use and would not be an ideal solution. Sentinel-2 is limited to a best-case temporal resolution of 5 days and so the UAV would be invaluable for capturing short term changes in target areas. The UAV is also excellent for monitoring vegetation post-treatment when it is greatly reduced as to not be visible by the Sentinel-2 MSI.

REFERENCES

Adams, D. C., & Lee, D. J. (2007). Estimating the Value of Invasive Aquatic Plant Control: A Bioeconomic Analysis of 13 Public Lakes in Florida. *Journal of Agricultural and Applied Economics*, *39*(s1), 97–109. https://doi.org/10.1017/S1074070800028972

Angle, S. (2019). Monitoring Yellow Floating Heart (Nymphoides peltata) on Lake Carl Blackwell via Remote Sensing. *ShareOK*.

Beets, J., & Netherland, M. (2018). Mesocosm response of crested floating heart, hydrilla, and two native emergent plants to florpyrauxifen-benzyl: A new arylpicolinate herbicide. *J. Aquat. Plant Manage.*, 6.

Belgiu, M., & Csillik, O. (2018). Sentinel-2 cropland mapping using pixel-based and object-based time-weighted dynamic time warping analysis. *Remote Sensing of Environment*, *204*, 509–523. https://doi.org/10.1016/j.rse.2017.10.005

Bradley, B. A. (2014). Remote detection of invasive plants: A review of spectral, textural and phenological approaches | SpringerLink. *SpringerLink*, *16*(7), 1411–1425. https://doi.org/10.1007/s10530-013-0578-9

Cacho, O. (2007). BIOECONOMICS OF INVASIVE SPECIES IN AQUATIC ECOSYSTEMS. *Aquaculture Economics & Mangement*, *10*(2), 107–124. https://doi.org/10.1080/13657300600695616

Cook, C. D. K. (1990). Seed dispersal of Nymphoides peltata (S.G. Gmelin) O. Kuntze (Menyanthaceae). *Aquatic Botany*, *37*(4), 325–340. https://doi.org/10.1016/0304-3770(90)90019-H

Darbyshire, S. J., & Francis, A. (2008). The Biology of Invasive Alien Plants in Canada. 10. Nymphoides peltata (S. G. Gmel.) Kuntze. *Canadian Journal of Plant Science*, *88*(4), 811–829. https://doi.org/10.4141/CJPS07208

Dash, J. P., Pearse, G. D., & Watt, M. S. (2018). UAV Multispectral Imagery Can Complement Satellite Data for Monitoring Forest Health. *Remote Sensing*, *10*(8), 1216. https://doi.org/10.3390/rs10081216

De Keukelaere, L., Sterckx, S., Adriaensen, S., Knaeps, E., Reusen, I., Giardino, C., … Vaiciute, D. (2017). Atmospheric correction of Landsat-8/OLI and Sentinel-2/MSI data using iCOR algorithm: Validation for coastal and inland waters. *European Journal of Remote Sensing*, *51*(1). Retrieved from https://www.tandfonline.com/doi/full/10.1080/22797254.2018.1457937

Duan, T., Chapman, S. C., Guo, Y., & Zheng, B. (2017). Dynamic monitoring of NDVI in wheat agronomy and breeding trials using an unmanned aerial vehicle. *Field Crops Research*, *210*, 71–80. https://doi.org/10.1016/j.fcr.2017.05.025

EO NASA. (2000). Measuring Vegetation (NDVI & EVI) [Text.Article]. Retrieved November 24, 2019, from https://earthobservatory.nasa.gov/features/MeasuringVegetation/measuring_vegetation_2.php

Epanchin-Niell, R., and Hastings, A. 2010. Controlling Established Invaders: Integrating Economics and Spread Dynamics to Determine Optimal Management. *Ecology Letters* 13 (4): 528–41. https://doi.org/10.1111/j.1461-0248.2010.01440.x.

Faidi, M. A., Hasan, M. G., & Shamsuddin, S. A. (2018). MAPPING OF LOTUS DISTRIBUTIONS USING SENTINEL-2 SATELLITE IMAGERY IN TASIK CHINI. *International Journal of Agriculture, Forestry, and Plantation*, *6*, 6.

Farid Muhsoni, F. (2018). COMPARISON OF DIFFERENT VEGETATION INDICES FOR ASSESSING MANGROVE DENSITY USING SENTINEL-2 IMAGERY. *International Journal of GEOMATE*, *14*(45). https://doi.org/10.21660/2018.45.7177

Gao, Y., Gao, J., Wang, J., Wang, S., Li, Q., Zhai, S., & Zhou, Y. (2017). Estimating the biomass of unevenly distributed aquatic vegetation in a lake using the normalized water-adjusted vegetation index and scale transformation method. *Science of The Total Environment*, *601–602*, 998–1007. https://doi.org/10.1016/j.scitotenv.2017.05.163

Gitelson, A. A., et al. "Vegetation and Soil Lines in Visible Spectral Space: A Concept and Technique for Remote Estimation of Vegetation Fraction." *International Journal of Remote Sensing*, vol. 23, no. 13, 2002, pp. 2537–2562., doi:10.1080/01431160110107806.

Harris GeoSpatial. (2019). Calculate Confusion Matrices. Retrieved from https://www.harrisgeospatial.com/docs/CalculatingConfusionMatrices.html

Henik, J. (2012). Utilizing NDVI and remote sensing data to identify spatial variability in plant stress as influenced by management. doi: 10.31274/etd-180810-2159

Hestir, E. L., Khanna, S., Andrew, M. E., Santos, M. J., Viers, J. H., Greenberg, J. A., … Ustin, S. L. (2008). Identification of invasive vegetation using hyperspectral remote sensing in the California Delta ecosystem. *Remote Sensing of Environment*, *112*(11), 4034–4047. https://doi.org/10.1016/j.rse.2008.01.022

Hill, D. J., Tarasoff, C., Whitworth, G. E., Baron, J., Bradshaw, J. L., & Church, J. S. (2016). Utility of unmanned aerial vehicles for mapping invasive plant species: a case study on yellow

flag iris (Iris pseudacorus L.). *International Journal of Remote Sensing*, *38*(8-10), 2083–2105. doi: 10.1080/01431161.2016.1264030

Howick, G. L., & Wilhm, J. (n.d.). *Turbidity in Lake Carl Blackwell: Effects of Water Depth and Wind*.

Huang, C., & Asner, G. P. (2009). Applications of Remote Sensing to Alien Invasive Plant Studies. *Sensors*, *9*(6), 4869–4889. https://doi.org/10.3390/s90604869

Husson, E., Ecke, F., & Reese, H. (2016a). Comparison of Manual Mapping and Automated Object-Based Image Analysis of Non-Submerged Aquatic Vegetation from Very-High-Resolution UAS Images. *Remote Sensing*, *8*(9), 724. https://doi.org/10.3390/rs8090724

Husson, E., Hagner, O., & Ecke, F. (2014). Unmanned aircraft systems help to map aquatic vegetation. *Applied Vegetation Science*, *17*(3), 567–577. https://doi.org/10.1111/avsc.12072

Jackson, R. D., Slater, P. N., & Pinter, P. J. (1983). Discrimination of growth and water stress in wheat by various vegetation indices through clear and turbid atmospheres. *Remote Sensing of Environment*, *13*(3), 187–208. https://doi.org/10.1016/0034-4257(83)90039-1

Joshi, C., Leeuw, J. de, & Duren, I. van. (2004). *Remote sensing and GIS applications for mapping and spatial modelling of invasive species*.

Kaplan, G., & Avdan, U. (2017). Object-based water body extraction model using Sentinel-2 satellite imagery. *European Journal of Remote Sensing*, *50*(1), 137–143. https://doi.org/10.1080/22797254.2017.1297540

Kettenring, K. M., & Adams, C. R. (2011). Lessons learned from invasive plant control experiments: A systematic review and meta-analysis. *Journal of Applied Ecology*, *48*(4), 970–979. https://doi.org/10.1111/j.1365-2664.2011.01979.x

Koenig, P. (2019). Herbicide Summary

Kovalenko, K. E., & Dibble, E. D. (2011). Effects of invasive macrophyte on trophic diversity and position of secondary consumers. *Hydrobiologia*, *663*(1), 167–173. https://doi.org/10.1007/s10750-010-0570-7

Lillesand, T. M., Kiefer, R. W., & Chipman, J. W. (2015). *Remote sensing and Image Interpretation*. Hoboken: John Wiley & Sons.

Lovell, S. J., Stone, S. F., & Fernandez, L. (2006). The Economic Impacts of Aquatic Invasive Species: A Review of the Literature. *Agricultural and Resource Economics Review*, *35*(1), 195–208. https://doi.org/10.1017/S1068280500010157

Lovett, G. M., Burns, D. A., Driscoll, C. T., Jenkins, J. C., Mitchell, M. J., Rustad, L., … Haeuber, R. (2007). Who needs environmental monitoring? *Frontiers in Ecology and the Environment*, *5*(5), 253–260. https://doi.org/10.1890/1540-9295(2007)5[253:WNEM]2.0.CO;2

Lukas, V., Novák, J., Neudert, L., Svobodova, I., Rodriguez-Moreno, F., Edrees, M., & Kren, J. (2016). *THE COMBINATION OF UAV SURVEY AND LANDSAT IMAGERY FOR MONITORING OF CROP VIGOR IN PRECISION AGRICULTURE*. 6.

Luo, J., Li, X., Ma, R., Li, F., Duan, H., Hu, W., … Huang, W. (2016). Applying remote sensing techniques to monitoring seasonal and interannual changes of aquatic vegetation in Taihu Lake, China. *Ecological Indicators*, *60*, 503–513. https://doi.org/10.1016/j.ecolind.2015.07.029

Ma, R., Duan, H., Gu, X., & Zhang, S. (2008). Detecting Aquatic Vegetation Changes in Taihu Lake, China Using Multi-temporal Satellite Imagery. *Sensors (Basel, Switzerland)*, *8*(6), 3988–4005. https://doi.org/10.3390/s8063988

Marbuah, G., Gren, I.-M., & Mckie, B. (2014). Economics of Harmful Invasive Species: A Review. *Diversity*, *6*(3), 500–523. doi: 10.3390/d6030500

Matese, A., Gennaro, S. F. D., Miranda, C., Berton, A., & Santesteban, L. G. (2017). Evaluation of spectral-based and canopy-based vegetation indices from UAV and Sentinel 2 images to assess spatial variability and ground vine parameters. *Advances in Animal Biosciences*, *8*(2), 817–822. https://doi.org/10.1017/S2040470017000929

McFeeters, S. (1996). The use of the Normalized Difference Water Index (NDWI) in the delineation of open water features: International Journal of Remote Sensing: Vol 17, No 7. *International Journal of Remote Sensing*, *17*(7), 1425–1432. https://doi.org/10.1080/01431169608948714

MicaSense. (2019, August 16). RedEdge-M User Manual (PDF). Retrieved from https://support.micasense.com/hc/en-us/articles/115003537673-RedEdge-M-User-Manual-PDF-

Minnesota Department of Agriculture. (2018). Florpyrauxifen-benzyl.pdf. Retrieved November 24, 2019, from https://www.mda.state.mn.us/sites/default/files/inline-files/Florpyrauxifen-benzyl.pdf

Müllerová, J., Pergl, J., & Pyšek, P. (2013). Remote sensing as a tool for monitoring plant invasions: Testing the effects of data resolution and image classification approach on the detection of a model plant species Heracleum mantegazzianum (giant hogweed). *International Journal of Applied Earth Observation and Geoinformation*, *25*, 55–65. doi: 10.1016/j.jag.2013.03.004

Nault, M. E., and A. Mikulyuk. 2009. Yellow Floating Heart (Nymphoides peltata): A Technical Review of Distribution, Ecology, Impacts, and Management. PUB-SS-1051. Wisconsin Department of Natural Resources.

OK EPSCOR, E. P. to S. C. R. (2019). Cimarron River Watershed Study Area | OK EPSCoR. Retrieved November 24, 2019, from http://www.okepscor.org/cimarron-river-watershed-study-area

Parker Williams, A., & Hunt, E. R. (2002). Estimation of leafy spurge cover from hyperspectral imagery using mixture tuned matched filtering. *Remote Sensing of Environment*, *82*(2), 446–456. https://doi.org/10.1016/S0034-4257(02)00061-5

Peñuelas, J., Gamon, J. A., Griffin, K. L., & Field, C. B. (1993). Assessing community type, plant biomass, pigment composition, and photosynthetic efficiency of aquatic vegetation from spectral reflectance. *Remote Sensing of Environment*, *46*(2), 110–118. https://doi.org/10.1016/0034-4257(93)90088-F

Pimentel, D., Zuniga, R., & Morrison, D. (2005). Update on the environmental and economic costs associated with alien-invasive species in the United States. *Ecological Economics*, *52*(3), 273–288. https://doi.org/10.1016/j.ecolecon.2004.10.002

Plants USDA. (2019). Plants Profile for Nymphoides peltata (yellow floatingheart). Retrieved November 24, 2019, from https://plants.usda.gov/core/profile?symbol=NYPE

Rahel, F. J. (2007). Biogeographic barriers, connectivity and homogenization of freshwater faunas: It's a small world after all. *Freshwater Biology*, *52*(4), 696–710. https://doi.org/10.1111/j.1365-2427.2006.01708.x

Seber, G. A. F., & Lee, A. J. (2012). *Linear regression analysis*. New York: Wiley.

SePro. (2019). ProcellaCOR®. Retrieved from https://www.sepro.com/aquatics/procellacor

Silva, T. S. F., Costa, M. P. F., Melack, J. M., & Novo, E. M. L. M. (2008). Remote sensing of aquatic vegetation: Theory and applications. *Environmental Monitoring and Assessment*, *140*(1), 131–145. https://doi.org/10.1007/s10661-007-9855-3

Simberloff, D. (2015). Non-native invasive species and novel ecosystems. *F1000Prime Reports*, *7*. https://doi.org/10.12703/P7-47

Smits, A. J. M., De Lyon, M. J. H., Van Der Velde, G., Steentjes, P. L. M., & Roelofs, J. G. M. (1988). Distribution of three nymphaeid macrophytes (Nymphaea alba L., Nuphar lutea (L.) Sm. And Nymphoides peltata (Gmel.) O. Kuntze) in relation to alkalinity and uptake of inorganic carbon. *Aquatic Botany*, *32*(1), 45–62. https://doi.org/10.1016/0304-3770(88)90087-3

Song, W., Mu, X., Ruan, G., Gao, Z., Li, L., & Yan, G. (2017). Estimating fractional vegetation cover and the vegetation index of bare soil and highly dense vegetation with a physically based method. *International Journal of Applied Earth Observation and Geoinformation*, *58*, 168–176. doi: 10.1016/j.jag.2017.01.015

Suhet. (2015). *Sentinel-2 User Handbook*. Retrieved from https://sentinel.esa.int/documents/247904/685211/Sentinel-2_User_Handbook

Summerfelt, R. C., & Shirley, K. E. (1978). *Environmental Correlates to Year-Class Strength of Largemouth Bass in Lake Carl Blackwell*. 11.

The Massachusetts Office of Coastal Zone Management. (2002). *MASSACHUSETTS AQUATIC INVASIVE SPECIES MANAGEMENT PLAN*.

Toetz, D., Bidwell, J., & Payton, M. (2009). Temporal and Spatial Variation in Stable Isotopes of Carbon and Nitrogen in Lake Carl Blackwell, Oklahoma: Journal of Freshwater Ecology: Vol 24, No 3. *Journal of Freshwater Ecology*, *24*(3), 461–467. https://doi.org/10.1080/02705060.2009.9664319

USDA APHIS. (2019). Plant Pests and Diseases. Retrieved November 24, 2019, from https://www.aphis.usda.gov/aphis/ourfocus/planthealth/plant-pest-and-disease-programs

USGA NAS. (2019). yellow floating-heart (Nymphoides peltata)—Species Profile. Retrieved November 24, 2019, from https://nas.er.usgs.gov/queries/FactSheet.aspx?speciesID=243

USGS EarthExplorer. (n.d.). EarthExplorer—Home. Retrieved November 24, 2019, from https://earthexplorer.usgs.gov/

Valta-Hulkkonen, K., Kanninen, A., & Pellikka, P. (2004). Remote sensing and GIS for detecting changes in the aquatic vegetation of a rehabilitated lake. *International Journal of Remote Sensing*, *25*(24), 5745–5758. https://doi.org/10.1080/01431160412331291170

Van Der Velde, G., & Van Der Heijden, L. A. (1981). The floral biology and seed production of Nymphoides peltata (GMEL.) O. Kuntze (Menyanthaceae). *Aquatic Botany*, *10*, 261–293. https://doi.org/10.1016/0304-3770(81)90027-9

Villa, P., Bresciani, M., Bolpagni, R., Pinardi, M., & Giardino, C. (2015). A rule-based approach for mapping macrophyte communities using multi-temporal aquatic vegetation indices. *Remote Sensing of Environment*, *171*, 218–233. https://doi.org/10.1016/j.rse.2015.10.020

Villa, P., Mousivand, A., & Bresciani, M. (2014). Aquatic vegetation indices assessment through radiative transfer modeling and linear mixture simulation. *International Journal of Applied Earth Observation and Geoinformation*, *30*, 113–127. https://doi.org/10.1016/j.jag.2014.01.017

Villa, P., Pinardi, M., Bolpagni, R., Gillier, J.-M., Zinke, P., Nedelcuţ, F., & Bresciani, M. (2018). Assessing macrophyte seasonal dynamics using dense time series of medium resolution satellite data. *Remote Sensing of Environment*, *216*, 230–244. https://doi.org/10.1016/j.rse.2018.06.048

Wang, J., Sun, L., & Liu, H. (2012). Monitoring biomass of water hyacinth by using hyperspectral remote sensing. *2012 First International Conference on Agro- Geoinformatics (Agro-Geoinformatics)*, 1–4. https://doi.org/10.1109/Agro-Geoinformatics.2012.6311673

Wang, L., Dronova, I., Gong, P., Yang, W., Li, Y., & Liu, Q. (2012). A new time series vegetation–water index of phenological–hydrological trait across species and functional types for Poyang Lake wetland ecosystem. *Remote Sensing of Environment*, *125*, 49–63. https://doi.org/10.1016/j.rse.2012.07.003

Willey, L., & Langeland, K. (2018). Aquatic Weeds: Crested Floating Heart (Nymphoides cristata). Retrieved November 17, 2019, from https://edis.ifas.ufl.edu/ag354

Xu, H. (2006). Modification of normalised difference water index (NDWI) to enhance open water features in remotely sensed imagery. *International Journal of Remote Sensing*, *27*(14), 3025–3033. https://doi.org/10.1080/01431160600589179

Zhonghua, W., Dan, Y., Manghui, T., Qiang, W., & Wen, X. (2007). Interference between two floating-leaved aquatic plants: Nymphoides peltata and Trapa bispinosa. *Aquatic Botany*, *86*(4), 316–320. https://doi.org/10.1016/j.aquabot.2006.11.008

VITA

Abigail A McCrea

Candidate for the Degree of

Master of Science

Thesis: ASSESSING THE USE OF IMAGERY FROM SENTINEL-2 AND AN UNMANNED AERIAL VEHICLE TO MONITOR NYMPHOIDES PELTATA IN AN OKLAHOMA RESERVOIR

Major Field: Environmental Science

Biographical:

Education:

Completed the requirements for the Master of Science in Environmental Science at Oklahoma State University, Stillwater, Oklahoma in May, 2020.

Completed the requirements for the Bachelor of Science in Environmental Science at Northern Michigan University, Marquette, Michigan in 2017.

Completed the requirements for a Geographic Information Systems Certificate at Northern Michigan University, Marquette, Michigan in 2017.

Professional Memberships:

Gamma Theta Upsilon
Mortar Board National College Senior Honor Society
Society of Environmental Scientists